SUPERCONDUCTIVITY, SPIN-GLASS PROPERTIES, AND FERROMAGNETISM IN AMORPHOUS La-Gd-Au ALLOYS

Thesis by

S. J. Poon

In Partial Fulfillment of the Requirements

for the Degree of

Doctor of Philosophy

California Institute of Technology

Pasadena, California

1978

(Submitted August 1977)

To My Parents

ACKNOWLEDGEMENTS

I wish to acknowledge Professor Pol Duwez for his constant support, advice and encouragement throughout this work. It has been a great pleasure to have been one of his students. I would like to express my sincere appreciation and thankfulness to Professor Bill Johnson and Dr. Jacques Durand who worked jointly with me in this work. Their abundant guidance, friendship and inspiration have been invaluable. I also remember Dr. C. C. Tsuei who introduced me to the fascinating field of superconductivity. I thank Angela Bressan, Sumio Kotake, Concetto Geremia, Joe Wysocki and Michael Yung for their friendship and technical assistance; and Vivian Davies for typing the final version of the manuscript. Besides science, the W. M. Keck Laboratory of Engineering Materials Group is also a haven of friendship and humanity. I am certain that I will remember my affiliation with the Keck Group as one of my best experiences.

Last, but not least, I would like to thank my parents for their continuous long-distance encouragement during the last six years. The financial support of the Energy Research and Development Administration is also gratefully appreciated.

ABSTRACT

The superconducting and magnetic properties of splat cooled amorphous alloys of composition $(La_{100-x}Gd_x)_{80}Au_{20}$ $(0 \leq x \leq 100)$ have been studied. The $La_{80}Au_{20}$ alloys are ideal type II superconductors (critical temperature $T_c = 3.5°$ K). The concentration range $(x < 1)$ where superconductivity and spin-glass freezing might coexist has been studied in detail. The spin-glass alloys $(0 < x < 70)$ exhibit susceptibility maxima and thermomagnetic history effects. In the absence of complications due to crystal field and enhanced matrix effects, a phenomenological model is proposed in which the magnetic clusters are treated as single spin entities interacting via random forces using the molecular field approach. The fundamental parameters (such as the strength of the forces and the size of clusters) can be deduced from magnetization measurements. The remanent magnetization is shown to arise from an interplay of the RKKY and dipolar forces. Magnetoresistivity results are found to be consistent with the aforementioned picture. The nature of magnetic interactions in an amorphous matrix is also discussed. The moment per Gd atom $(7\mu_B)$ is found to be constant and close to that of the crystalline value throughout the concentration range investigated. Finally, a detail study is made of the critical phenomena and magnetic properties of the amorphous ferromagnet: $Gd_{80}Au_{20}$. The results are compared with recent theories on amorphous magnetism.

TABLE OF CONTENTS

Table of Contents (Cont'd)

LIST OF FIGURES

List of Figures (Cont'd)

LIST OF TABLES

I. INTRODUCTION

Recently, magnetism and superconductivity in amorphous alloys have become a fashionable area of research. These alloys have attracted a great deal of interest in the fundamental studies of solid state physics and technological applications. More than two decades ago, Buckel and Hilsch[1] from Göttingen discovered the first thin film amorphous superconductors of bismuth and gallium. Since then, both soft metal and transition metal amorphous superconductors had been prepared by quench condensation.[2] Results of superconducting tunneling experiments, upper critical field measurements and far infrared absorption were reported. Meanwhile there were theoretical attempts to understand amorphous superconductivity, particularly the problem of electron-phonon interaction in disordered materials. A few years ago, the first series of bulk amorphous superconductors obtained by liquid quenching was reported.[3] Based on the unique transport properties of these alloys, their possible technological applications were suggested.

A long time ago, it was discovered that superconductivity can be easily destroyed by introducing magnetic impurities in superconductors.[4,5] It was believed that the conduction-electron-impurity-spin exchange interaction could account for the strong depression of T_c. Within the first Born approximation (to second order in the exchange constant J), Abrikosov and Gor'kov (AG) developed[6] a classic theory for superconductors with paramagnetic impurities. Their theory successfully explained some of the basic features of the

early experiments, one of which is that the superconductors are gapless. Our discussion will be mainly concerned with magnetic impurities possessing long-life local moments (i.e., the spin fluctuation time τ_{sf} tends to infinity). However, significant departures from the AG theory were also observed in many alloy-impurity systems. Cumulating numerous experimental and theoretical results over a decade, it was found that the depression of T_c depends on the magnetic states of the impurities.[7] Those in the single impurity (Kondo) state , antiferromagnetic or ferromagnetic states all affect T_c differently. We shall mention some of the most famous theoretical work. There was the Müller-Hartman-Zittartz theory[8] which predicted "reentrant" behavior in Kondo superconductors. Bennemann[9] was the first one to discuss deviations from the AG behavior due to magnetic interactions. Using only the mean exchange field approach, his theory did not include spin-spin correlations. The theories of Entel and Klose[10], and Rainer[11] did include spin correlations and were more capable of describing the experimental results. Today, with a better understanding of the different types of magnetic ordering, the coexistence of superconductivity and "spin glass freezing" was suggested for several of the previously investigated systems.[12,13] However, a clear picture of the spin dynamics in the freezing process (defined by a sharp susceptibility maximum) is required before we can understand the so-called "coexistence" phenomenon. Therefore we should focus on the magnetic properties for a moment.

Spin glass properties in dilute magnetic alloys containing 3d-magnetic solutes have been studied quite extensively.[14] The indirect

Ruderman-Kittel-Kasuya-Yosida (RKKY) interaction[15] between the pairs of magnetic impurities in host metals via the host conduction electrons is believed to play an important role on the observed magnetic properties in spin-glasses. Based on the $1/r^3$ dependence of the RKKY interaction, scaling predictions[16] for the various thermodynamic parameters were made. Results of specific heat and magnetization measurements in canonical spin-glasses (e.g., AuFe and CuMn dilute alloys[17]) follow the scaling laws reasonably well. This constitutes an additional evidence for the $1/r^3$ dependence of the indirect s-d exchange interaction. Recently we have studied the magnetic superconducting properties of dilute amorphous La-Au-Gd alloys. This study serves two purposes. First, investigation on the rare-earth spin-glasses has been a very recent event.[18] It is believed that the s-f interaction is weaker than the s-d interaction. In addition, this interaction is expected to be significantly attenuated in an amorphous matrix, as the electronic mean free path reaches a few interatomic spacings.[19] All these should be reflected in the magnetic properties of our alloys. Second, the magnetic state of Gd impurities will be manifested in the depression of T_c as discussed beforehand. This allows a comparison of consistency with the magnetic measurements of the alloys. It should also be mentioned that using Gd (S-state ion) can eliminate the complications due to crystal field effects.

As one keeps adding magnetic impurities to a normal matrix, complex magnetic regimes appear. Many investigators have studied the complex regimes which occur between the Kondo state and the

long-range magnetic order in crystalline[20] normal matrix with 3d impurities for at least fifteen years. Similar investigation on the amorphous state has been relatively recent.[21] Basic phenomena such as susceptibility maxima at low field, isothermal and thermal remanent magnetizations, thermal history effects, and resistivity minima are rather common in these alloys. Apart from the different terminologies such as "spin-glass" or "mictomagnet" (meaning mixed magnetism) which have been given to these alloys, the basic physics is always dealing with a competition between antiferromagnetic and ferromagnetic alignments of the spins intervening by some sort of anisotropy force. One realizes that once the magnetic states in the dilute alloys (above the Kondo critical concentration) are known, which is the simplest case, a significant progress has been made. There have been close to a few dozen theoretical treatises on this subject in the past few years, the main ones of which will be reviewed in a later section. Our purpose of studying the complex regime ($1.25 < x < 70$) is to investigate the spin-glass mechanism in concentrated alloys based on our understanding of the dilute regime. We would also like to find out the critical concentration at which the magnetic properties can no longer be described by simple laws. Then, the approach to ferromagnetism can be understood from such analysis. Besides magnetization studies, transport properties of alloys in the spin-glass regime have also been investigated. The latter serves as an additional tool for probing the magnetic states of the alloys.

In amorphous ferromagnets, there was a basic problem of whether or not a second order magnetic phase transition can exist in

random systems. Theoretical investigations using renormalization group analysis and cumulant expansion technique in the Ising spin models and isotropic Heisenberg spin models were made for these systems.[22] Criteria for observing a sharp transition in a random alloy were discussed. Meanwhile, magnetization and specific heat measurements were carried out[23] on splat-cooled amorphous transition metal alloys. For some of the systems studied, particularly the Co-P-B, Fe-P-C and Metglass 2826A alloys, the results indicated a sharp transition with well-defined critical exponents. The reduced magnetization and field satisfy an equation of state derived for second order phase transition in fluid systems[24], with the critical exponents satisfying an equality relation. Similar to the crystalline cases, the materials studied have critical exponents quite close to the theoretical values derived from the Heisenberg model.

In amorphous transition-metal alloys where the d-electrons play a significant role on their magnetic states, the amorphous ferromagnetism is discussed in terms of a distribution of the Heisenberg exchange interaction.[25] There exist other microscopic theories[26] which predict the magnetic properties of disordered alloys using the site diluted or bond random models. In the rare-earth transition-metal alloys (such as $HoFe_2$ and $TbFe_2$), it is suggested[27] that the RKKY exchange interaction between the magnetic atoms is constant and the amorphous nature of the alloy is manifested in a random distribution of local anisotropy field. However, the situation might be different in our amorphous Gd-Au alloys where Gd is an S-state ion. The anisotropy field effect is expected to be small and one can focus

on the other effects of amorphousness on the magnetic properties.

We have studied the magnetic properties of bulk amorphous $Gd_{80}Au_{20}$ alloys obtained by liquid quenching. A detailed study is made on the critical behavior of amorphous $Gd_{80}Au_{20}$ alloys around its Curie temperature T_c. We have determined the spontaneous magnetization and initial susceptibility values in the critical region. This allows determination of the critical exponents and T_c. Magnetization results of single crystal Gd[28] were found to depend strongly on the crystal axis along which the field was applied. Measurements on amorphous Gd are expected to yield an averaged result of the corresponding crystalline values. Possible asymptotic equations of state are to be investigated following the work of Kouvel and Comly.[29] An attempt is made to compare the results of different amorphous alloys with existing theories on the critical behavior of disordered systems. The roles played by different forces in the vicinity of Curie transition are also considered. We have also studied the effect of structural randomness on the magnetic properties (effective moment μ_{eff}, saturation moment μ_{Gd}, T_c, spontaneous magnetization $M_s(T)$, and saturation magnetization $M(\infty,T)$) of $Gd_{80}Au_{20}$. Comparison of the present results with those of crystalline compounds and solid solutions is made. These results are extrapolated to the case of pure amorphous Gd and compared with theoretical predictions whenever possible.

A. A Historical Perspective: From Rock Magnetism to Spin-Glass

The term "spin-glass" was recently introduced by B. R. Coles[14] to describe a class of alloys which exhibit unusual "magnetic freezing" behavior. Historically, such a phenomenon is much older than the terminology itself. About a century ago, J. Hopkinson[30] discovered that the magnetic susceptibility of coarse grained basalt containing magnetic inclusions decreased substantially below a characteristic temperature T_B, while it showed the normal paramagnetic behavior above T_B (Fig. 1). However, the subject of rock magnetism did not attract the attention of solid state physicists until the first pioneering work of Néel.[31] Néel studied the superparamagnetic properties of small particles and of their blocking temperatures where the rapid spin fluctuation is frozen into a stable configuration below a characteristic temperature. The theory can be extended to a system of small particles having a spectrum of blocking temperatures. It was suggested that the existence of anisotropy of some sort could account for the freezing phenomenon.

Later on, maxima in the susceptibility and specific heat were also observed in dilute alloys.[32] In addition, a small remanent magnetization was observed at temperatures below that of the susceptibility manimum after application of a magnetic field. The qualitative properties of this remanence are its saturation at sufficiently high fields, its decay with time, and its marked increase at lower temperatures. To account for the maxima in the specific heat and susceptibility, Klein and Brout[33] presented a statistical

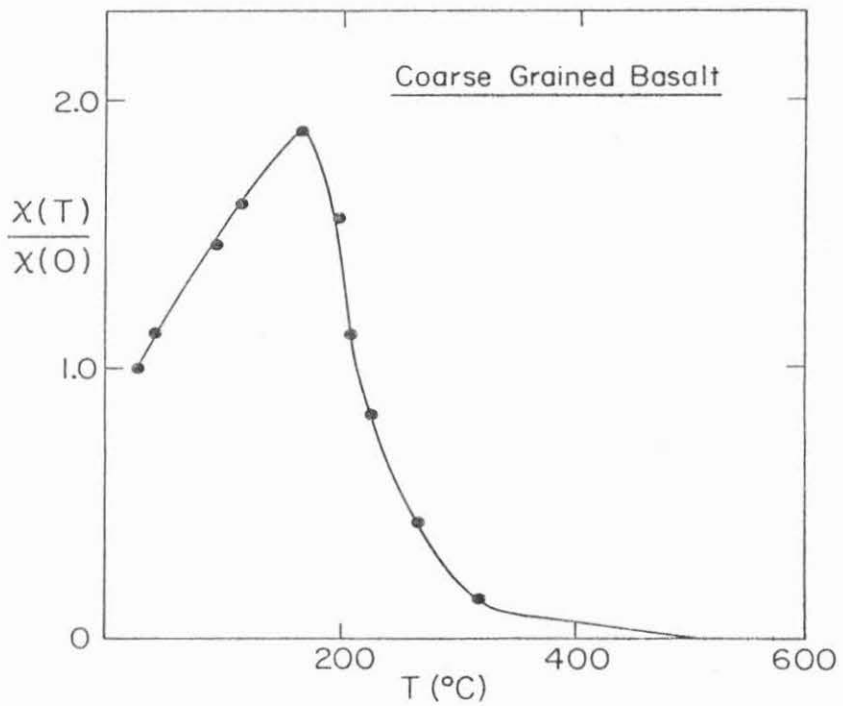

Fig. 1. Temperature dependence of the susceptibility of a coarse grained basalt.

mechanics model of dilute CuMn alloys. Using an indirect "Ising model" interaction between the magnetic impurities, it was shown that the system was composed of small clusters of spins (not chemical clusters) that were strongly correlated to each other within a cluster, but various clusters were randomly orientated relative to each other. An impurity within each cluster found itself in an average "local effective field," the probability distribution of which was also obtained. As the temperature was increased, the internal structure of the clusters was broken up, and at higher temperatures, the system exhibited paramagnetic behavior. Although this model could explain the main features in the specific heat and susceptibility experiments, yet it did not (even to date) describe the remanent magnetizations.

Meanwhile, a more phenomenological model to explain the remanence and susceptibility maximum was proposed by J. S. Kouvel.[33] The magnetic structure at low temperatures was simulated by a simple model in which the magnetic unit is composed of mutually-interacting ferromagnetic and antiferromagnetic domains. In the ground state, each domain-ensemble has zero net magnetization, but when the system is cooled in a magnetic field some of its domain-ensembles are forced into a different state (with nonzero magnetization) which is stabilized by the growth of strong anisotropy in the anti-ferromagnetic domains. Using this model, a magnetic hysteresis loop displaced asymmetrically from the origin (observed experimentally) and the susceptibility maximum were reproduced. We shall demonstrate schematically the magnetization process in the following

(Figure 2). At point P, the sample is cooled in a magnetic field below the blocking temperature* (onset of anisotropy). Each ensemble in the matrix is composed of ferromagnetic (F) and antiferromagnetic (A) regions. Regions F are coupled to region A through exchange interactions which are responsible for the remanent magnetizations at decreasing field (point Q). In reversing the field, the F-domain moments will rotate in unison from their remanence directions. So will the A-domain moments owing to their net coupling with adjacent F-domains. However, if there exists a strong anisotropy force which locks the A-domains in the original field-cooled direction, and if this force is large compared to the net exchange couplings between A- and F-domains, the angle Φ will remain small regardless of the direction of the F-domain magnetization. Consequently, the net coupling force opposing the external field will tend to hold the F-domain magnetization in the original remanence direction (point R) until the reverse field reaches a critical value $-H_c$, at which point they will reverse their direction (point S). Moreover, when the reverse field is reduced through the same critical value, the magnetization will revert to their original orientation (point R). Therefore H_c acts like a negative biasing field on the ferromagnetic domains. In Fig. 2 is also shown a zero-field cooled hysteresis loop below T_B.** As opposed to the field-cooled

---

*This is the experimental procedure for obtaining thermal remanent magnetization (known as TRM). One cools the sample from $T > T_B$ to $T < T_B$ in a magnetic field so as to align the anisotropy axes along the field.

**This is known as the isothermal remanent magnetization (IRM). One cools the sample to $T < T_B$ at zero field. The IRM is then obtained at T by applying a field.

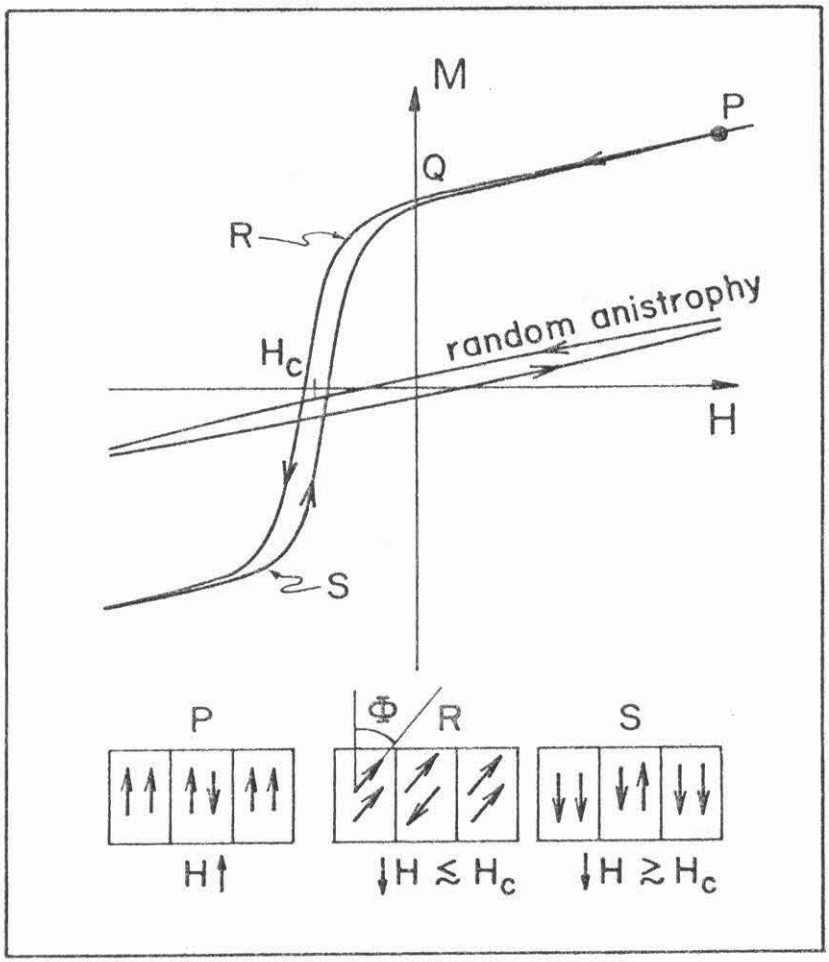

Fig. 2. Schematic hysteresis loops for alloys cooled in a positive field and in zero field.

case, the anisotropy axes are now locked along random directions thus giving rise to zero remanence and a symmetric loop. What about the nature of anisotropy? It may originate from cluster shape, stresses on clusters or the anisotropic part of the interactions (dipole-dipole, RKKY, crystal-field, etc.) between the clusters, still to be investigated.

In the early seventies, the concept "spin-glasses" was introduced to describe the freezing phenomena in dilute systems, such as CuMn, and AuFe.[34] The use of this fashionable name is related to the growing interest in problems dealing with amorphous and disordered systems. At about the same time, the term "mictomagnet" (in Greek, micto means mixed) was introduced by P. Beck[20] for concentrated alloys exhibiting similar phenomena. A typical result of Ref. 34 is reproduced in Fig. 3. Today, ingenious mathematical and computational techniques are used to obtain significant physical results. However, further effort is required to understand the different phenomena in a consistent fashion. Specifically, questions concerning the reconciliation of a sharp cusp in the susceptibility and the absence of long-range magnetic ordering, the relation between the sharp cusp and the onset of anisotropy, spin waves in spin-glasses, have to be answered. So far, one has to say that the work on spin-glasses has had a significant impact on the study of magnetism in amorphous systems.

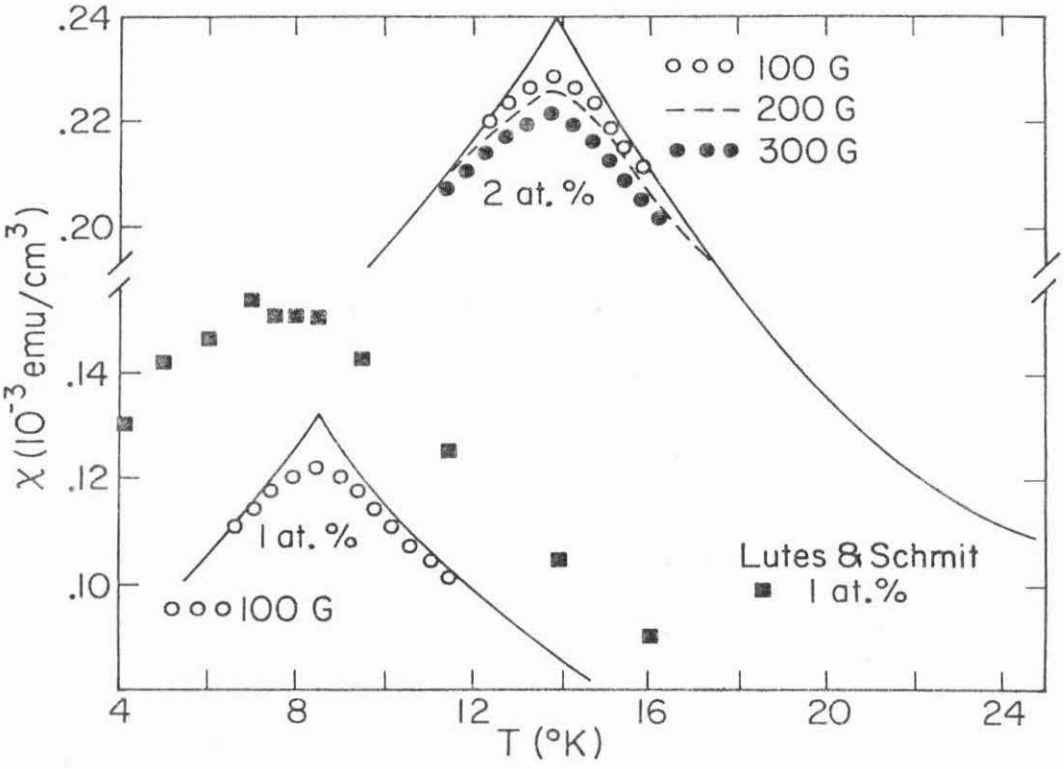

Fig. 3. Susceptibility vs. temperature for samples with 1 and 2 at.% Fe. Data taken from reference 34.

II. EXPERIMENTAL PROCEDURES

The purity of La and Gd used in this study is 99.9+ %. Alloys of composition $(La_{100-x}Gd_x)_{80}Au_{20}$ with x = 0, 0.3, 0.5, 0.62, 0.7, 0.75, 0.8, 0.85, 1.25, 5, 8, 12, 16, 20, 34, 40, 50, 56, 60, 70, 80 and 100 were prepared by induction melting of the appropriate constituents on a silver boat under an argon atmosphere. Samples were then quenched from the liquid state using the "piston and anvil" technique described in Ref. 35. The cooling rate is estimated to be of the order 10^6 °C/sec. Samples prepared by this technique were in the form of foils with surface area of ~ 2 × 2 cm^2 and thickness of about 40 μ m. The structure of each sample was checked by X-ray scanning with a Norelco diffractometer. Only samples containing a single amorphous phase were retained for detailed experimental studies The X-ray patterns (Cu Kα) of the samples were characterized by a broad maximum the center of which ranges from 30.7° in $La_{80}Au_{20}$ to 32.8° in $Gd_{80}Au_{20}$ with a full width at half maximum of ~ 4.6°. According to the Sherrer formula, this corresponds to an effective microcrystal size of ~ 17 Å, which is typical of a glassy metal. No significant annealing effect is observed for the amorphous phases at room temperature during periods of several weeks. Spontaneous crystallization is observed at temperatures of about 150 to 200° C.

Magnetization measurements as functions of magnetic field (up to 75 kOe) and temperature (1.8° K to 290° K) were carried out by using the Faraday method with an Oxford Instruments Magnetometer described previously.[36] Samples used in the M(H, T) measurements were in the form of disks (3 mm in diameter) punched from foils.

The thermal output controls have an accuracy of ~ 0.05° K. Magnetic ordering temperatures were observed using a standard ac inductance bridge technique. Resistivity measurements were performed by using the standard four-probe technique over a temperature range of 1.3 - 270° K in zero field, and 2 - 40° K in transverse fields up to 40 kOe. The resolution of the measurements was 1 part in 10^5. For the $Gd_{80}Au_{20}$ samples, measurements for M(H) were made approximately every 20° K from 4° K to 290° K and for fields up to 70 kOe. Near the Curie point (~ 149° K), measurements were made every 1° K in the temperature range of 136° K to 160° K, and for fields up to 40 kOe.

III. RESULTS, ANALYSIS AND DISCUSSION

Most of the experimental results cited in this work have been presented in our previous publications henceforth referred to as P{i} (i = 1, 2, ... 6) in the text. This thesis contains mainly materials which are not covered in P{i}. These include a general view of the fundamental concepts mentioned but not discussed in the previous work, a phenomenological spin-glass model for concentrated alloys, and the effect of amorphousness on the magnetic interactions. The readers are urged to review the relevant materials covered in P{i} in order to get familiarized with the experimental results frequently referred to in this work. Convenient references to P{i} are made in the text.

PUBLICATIONS

P1. "Amorphous superconducting lanthanum-gold alloys obtained by liquid quenching" W. L. Johnson, S. J. Poon and P. Duwez, Phys. Rev. B11, 150 (1975)

P2. "The Ruderman-Kittel-Kasuya-Yosida Interactions in Amorphous $La_{80}Au_{20}$ Alloys with Dilute Gd Impurities" S. J. Poon and J. Durand, Solid State Commun. 21, 793 (1977)

P3. "Superconductivity and Spin-Glass Regime in Amorphous $La_{80}Au_{20}$ Alloys Doped with Gd" S. J. Poon and J. Durand, Solid State Commun. 21, 999 (1977)

P4. "Remanent Magnetization of Amorphous La-Gd-Au Alloys with High Gd Content" S. J. Poon and J. Durand, to be published in Communications on Physics, 1977

P5. "Magnetic Field Dependence of Resistivity Minima in Amorphous La-Gd-Au Alloys with High Gd Content" S. J. Poon, J. Durand and M. Yung, Solid State Commun. 22, 475 (1977)

P6. "Critical Phenomena and Magnetic Properties of an Amorphous Ferromagnet: Gadolinium-Gold" S. J. Poon and J. Durand, to be published in Physical Review B, July 1, 1977

A. DILUTE ALLOYS ($0 \leq x \leq 1.25$)

1. Amorphous $La_{100-x}Au_x$ ($18 \leq x \leq 26$) Superconductors

The critical behavior and transport properties of amorphous superconducting $La_{80}Au_{20}$ alloys have been discussed in publication P1. To summarize: These alloys are ideal type II superconductors (i.e., without flux pinning) characterized by $T_c \simeq 3.5°$ K, $H_{c2}(0) \simeq 60$ kOe, $\xi(0) \simeq 60$ Å, $J_c(0) \simeq 10^4 A/cm^2$ and a Ginsburg-Landau parameter K of ~ 70. Spin-orbit scattering effects are found to be stronger in the amorphous samples than in disordered crystalline samples. Such phenomena are common in amorphous superconductors.[2] Here, we would like to comment on the values of the electronic diffusivity D_e determined in P1. One uses a relation between D_e and resistivity ρ

$$D_e = m^* V_F^2 / 3ne^2\rho = 2E_F/3ne^2\rho \qquad (1)$$

Then a value $D_e \simeq 1.00$ cm^2/sec is obtained as shown in P1. However, the diffusivity determined from the $H_{c2}(t)$ relation is a "dressed" diffusivity D_λ given by

$$D_\lambda = D_e/(1 + \lambda) \qquad (2)$$

since the electronic energy has to be renormalized, where λ is the

electron-phonon coupling parameter defined by McMillan.[37] Taking $\lambda \simeq 1.0$ as will be justified later, one sees immediately that D_λ determined from (2) agrees well with that determined from $H_{c2}(t)$.

More experiments have been performed on these bulk amorphous superconductors. Johnson and Tsuei[38] investigated fluctuation conductivity in three-dimensional amorphous superconductors. They observed a rather universal temperature dependence of the fluctuation conductivity for a wide variety of bulk amorphous superconductors. The theoretical predictions of the Aslamasov-Larkin (AL) theory were found to provide a quantitative account of the data near T_c.

Recently, Shull and Naugle[39] reported low temperature specific heats measurements of amorphous $La_{80}Au_{20}$ alloys. The normal state data can be fitted to the usual T plus T^3 law. The Debye temperature was ~ 100° K (~ 142° K in pure La) which indicated a significant softening of phonon modes. The constant $\gamma \simeq 8.1$ m J/mole K^2 is also lower than that of pure La. The coupling parameter λ was estimated to be ~ 0.89 which can only be classified as intermediate coupling superconductors. More specific-heat experiments on La-X amorphous superconductors are under way to probe the variation in the density of states and Debye temperature as a function of X species and concentrations.

We have obtained magnetization results between 1.7° K and 290° K for the $La_{80}Au_{20}$ alloys. This allows us to determine the temperature-independent band contribution susceptibility χ' and the

magnetization due to magnetic impurities in the alloys. The raw data are shown in Fig. 4. It can be seen that at 1.8° K, the upper critical field is about 40 kOe. At this point, it is worthwhile to mention a standard method of analyzing the magnetization data. This method will be widely used in later sections. In the presence of magnetic impurities, the initial susceptibility χ_o can be expressed by the phenomenological law

$$\chi_0(T) = \chi' + C_{cw}/(T + \theta) \tag{3}$$

where C_{cw} is the Curie-Weiss constant, θ is some characteristic temperature (can arise from Kondo effect, magnetic interaction, spin fluctuation, etc.). In the case of small θ, one can plot $\chi_0 T$ vs. T which gives a straight line at $T >> \theta$. χ' is then given by the gradient of the straight line and C_{cw} is determined from its intercept at T = 0. Such plot is made for $La_{80}Au_{20}$ in Fig. 5. It is found that $C_{cw} = 7.5 \times 10^{-6}$ cgs and $\chi' \simeq 0.5 \times 10^{-6}$ cgs which can be compared with the dHCP La $\chi' = 0.7 \times 10^{-6}$ cgs.[40] The magnetization can then be decomposed into two parts

$$M(H, T) = M_{mag}(H, T) + \chi' H \tag{4}$$

where $M_{mag}(H, T)$ is the magnetic impurities contribution to the total magnetization. One then can estimate the average impurity concentration $\bar{c}$ and the average magnetic spin $\bar{S}$ from C_{cw} and the saturation $M_{mag}(\infty, 1.8)$. The latter quantities give $C_{cw} = \bar{c} N g^2 \mu_B \bar{S}(\bar{S} + 1)/3k_B$ (N = Avogadro's Number, g = spectroscopic splitting factor) and

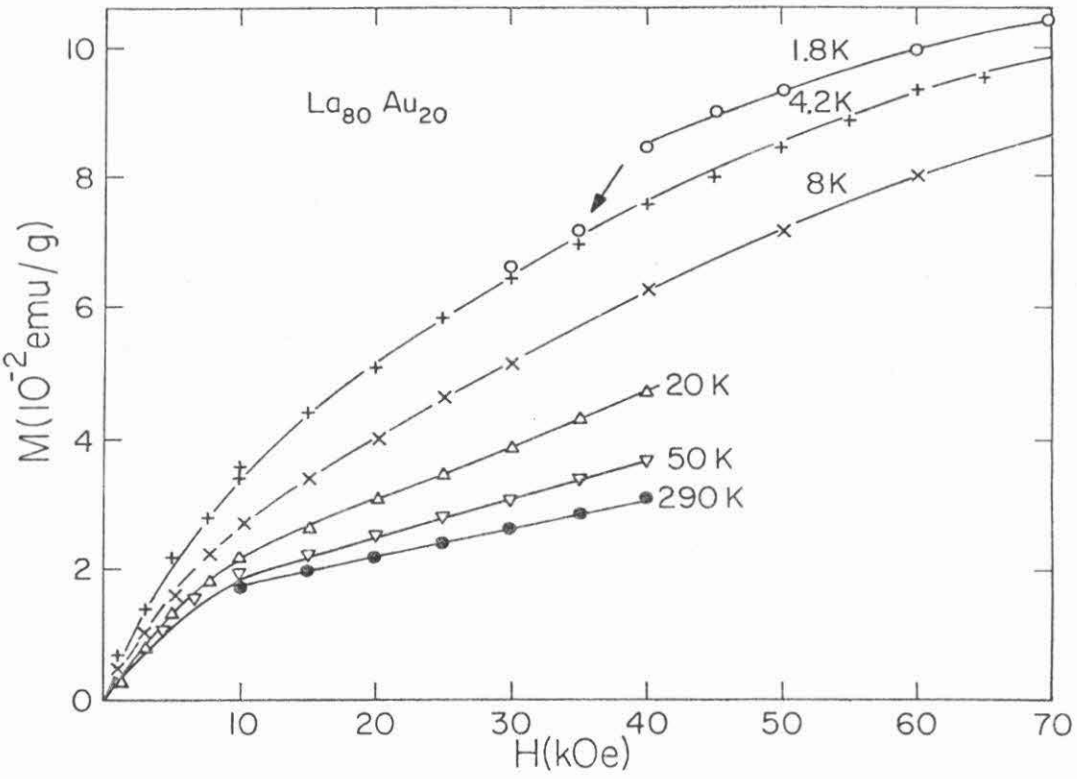

Fig. 4. Magnetization vs. applied field for $La_{80}Au_{20}$ at low temperatures. The arrow indicates the upper critical field value at 1.8 K.

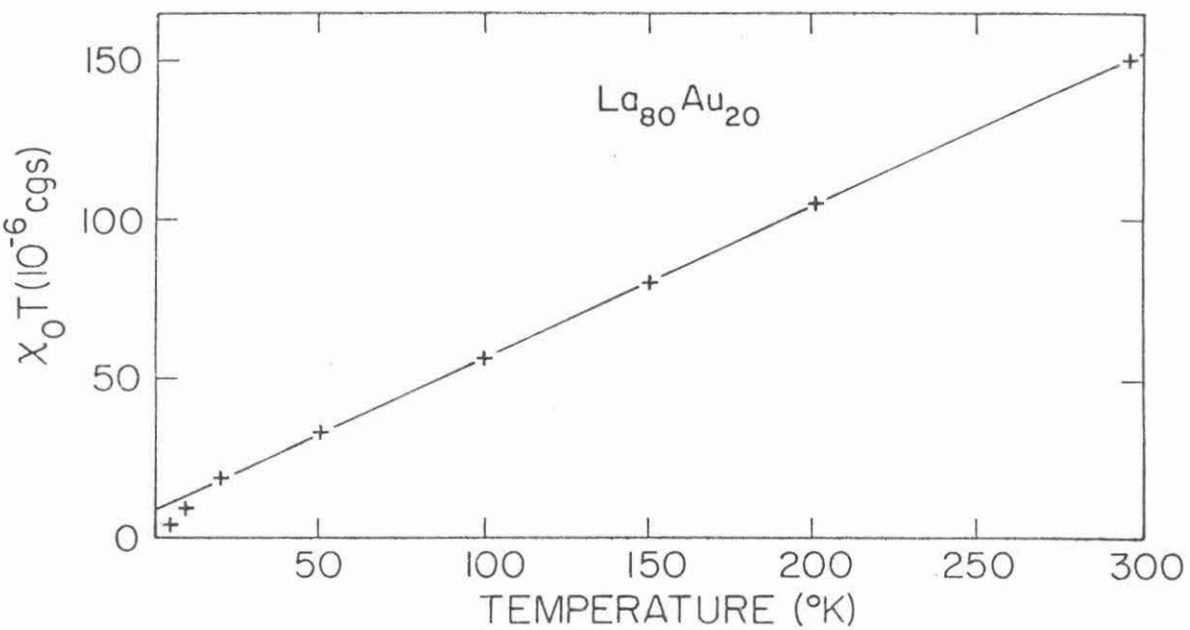

Fig. 5. $\chi_o T$ vs. temperature for $La_{80}Au_{20}$.

$M_{mag}(\infty, 1.8) = \bar{c}Ng\mu_B\bar{S}$. For the $La_{80}Au_{20}$ alloys, $M_{mag}(\infty, 1.8) \simeq 6 \times 10^{-2}$ emu/g. Using the C_{cw} value determined beforehand, we obtain $\bar{c} \simeq 350$ ppm and $\bar{S} \simeq 2.25$. The $\bar{S}$ value so determined is that one would expect from the list of abundance of magnetic impurities (mainly Fe, Gd, Nd) in La given in Ref. 40.

2. Canonical Spin-Glass and Magnetic Interaction

The magnetization data are analyzed in the same way as discussed above. Values of $M_{mag}(\infty, 1.8°)$ and C_{cw} vs. Gd composition x are shown in Fig. 6. The intercepts at $x \to 0$ yield values which agree reasonably well with those determined for the matrix. The linear relations also verify indirectly the nominal compositions. The $1/r^3$ dependence of the interaction among the localized 4f spins and the strength of the interaction are discussed in P2. In amorphous materials, the electronic mean free path ℓ_{mfp} is on the order of interatomic distance ($\rho \sim 100\ \mu\Omega$cm). This effect certainly plays a crucial role on the indirect interactions.[19] Unfortunately, this point was not discussed in P2. It is interesting to note that the results we obtained can be analyzed in the same way as in crystalline alloys (where $\ell_{mfp} \gtrsim 100$ Å). In this section, we shall try to discuss this point in greater depth. Before doing so, let us first review the fundamental basis of the scaling laws of Blandin, Souletie and Tournier.[16]

a. The Scaling Laws of Blandin, Souletie and Tournier. The interaction between the magnetic moment μ on impurities in an alloy has the well-known form[15,41]: $\cos(2k_F r + \Phi)/r^3$ which is the

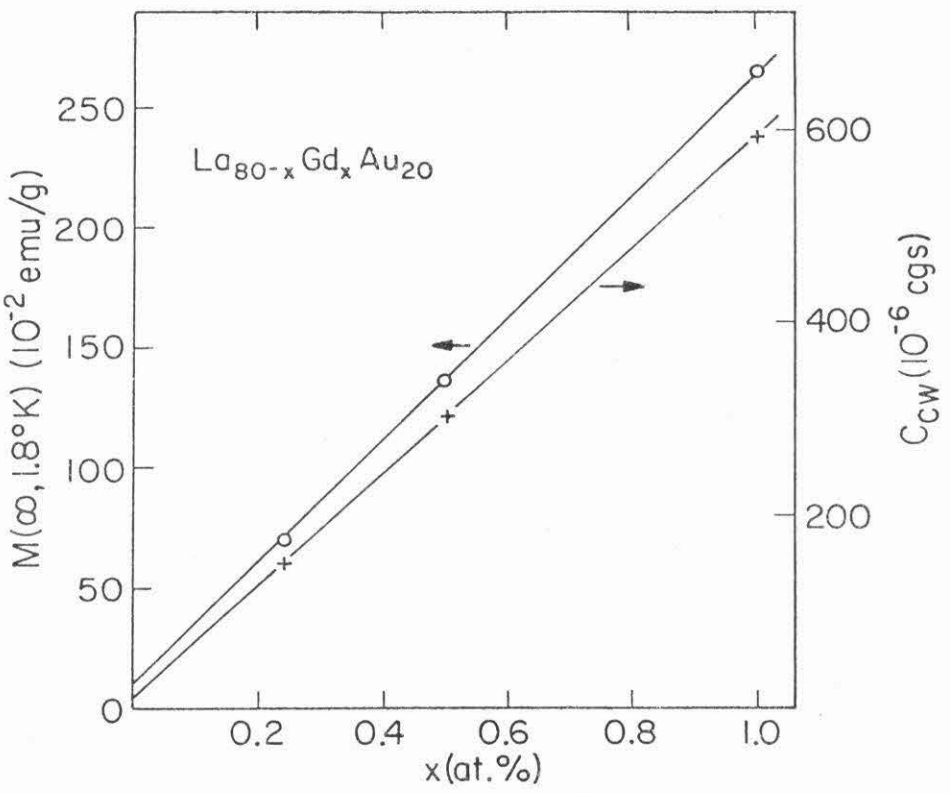

Fig. 6. Compositional variations of M(∞, 1.8 K) and C_{CW} for $La_{80-x}Gd_xAu_{20}$ ($x \leqslant 1$) alloys.

asymptotic behavior of the RKKY function $F(x) = (x \cos x - \sin x)/x^4$. This approximation is valid since the wavelength of the oscillation is small ($2k_F a = 6.92$ for Ag, Au, or Cu, where a is the distance between first neighbors). In the Ising molecular field model, all spins are supposed to be oriented parallel or antiparallel to a fixed direction. The field acting on a spin at site i is given by

$$h_i = V_o \sum_{j \neq i} S_j \frac{\cos(2k_F r_{ij} + \Phi)}{r_{ij}^3} \tag{5}$$

where V_o is the strength of the interaction. From first sight, such an Ising representation would seem rather restrictive, but it makes the formulation easier and in some cases, the calculation possible. However, the geometrical argument proposed for the scaling laws is of wider generality and can be easily extended to a three-dimensional model.[42]

Suppose when the concentration c of a dilute alloy is reduced to c', we change the unit of measurement of distance from r to r', where $cr^3 = c'r'^3$ so that we have the same number of particles in the new volume. It is obvious then to modify the expression of the molecular field to

$$\frac{h_i}{c} = V_o \sum_{j \neq 1} S_j \frac{\cos(2k_F r_{ij} + \Phi)}{c r_{ij}^3} \tag{6}$$

In a statistical calculation where a large number of impurities are distributed randomly in the matrix, the role of the cosine function will be sufficiently characterized by the moments of this function, provided

its wavelength remains small compared with the distances between impurities (Fig. 7). Thus the solutions in h/c of the molecular field are possible solutions of any other very low concentration c'. We now define a probability distribution function P(h) by $\frac{1}{N}\int_{-\infty}^{\infty} P(h)dh = 1$ for a given number of impurities. So $P(h) = dN(h)/dh$ which can be rewritten as

$$P(h) = \frac{dN(h)}{d(h/c)} \times \frac{1}{c}$$

$$cP(h) = f(h/c) \tag{7}$$

The last step comes from the fact that N(h) is a function of h/c only, for a given number N. Thus f is a function independent of concentration.

The function P depends on external field H and temperature T through $S_i(H, h, T)$. The latter being given by a Brillouin function $B_s\left[\frac{S(H+h)}{k_B T}\right]$ which is again independent of concentration. Thus at a given T/c and H/c, we have

$$cP(h, T, H) = f(h/c,\ T/c,\ H/c) \tag{8}$$

Consequently the energy of the magnetic impurities in a given volume V can be written

$$E = -\frac{1}{2} \times \frac{cV}{N} \int_{-\infty}^{\infty} P(h, T, H) \mathcal{S}(H+h)\, B_s\left[\frac{S(H+h)}{k_B T}\right] dh =$$

$$= -\frac{1}{2} \times \frac{c^2 V}{N} \int_{-\infty}^{\infty} f\left(\frac{h}{c},\ \frac{T}{c},\ \frac{H}{c}\right) B_s\left[S\,\frac{(H/c + h/c)}{k_B (T/c)}\right] \mathcal{S}(H+h)\,\frac{dh}{c} \tag{9}$$

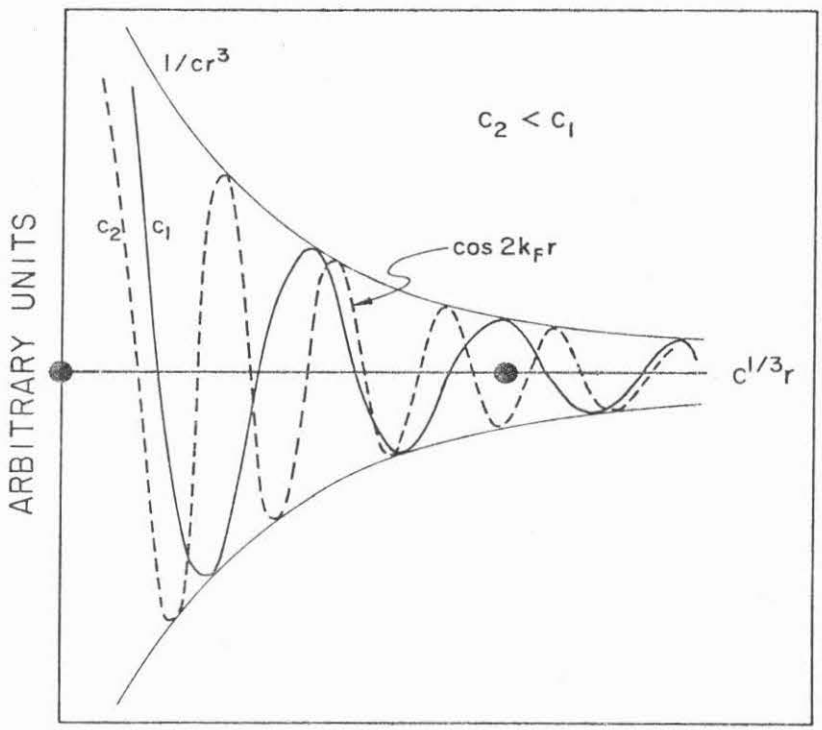

Fig. 7. Schematic dependence of RKKY interaction on scaled distance $c^{1/3}r$ for two concentrations. The magnetic atoms are represented by filled circles. The number of angular cycles separating the atoms in each case should be noted.

from (8). After integrating over all the values of the molecular field h,

$$E = c^2 \Phi\left(\frac{T}{c}, \frac{H}{c}\right) \tag{10}$$

From the energy functional, the magnetic contribution to specific heat $C_m = C_{alloy} - C_{matrix}$ can be obtained.

$$C_m(T, H) = \frac{\partial E}{\partial T} = C\Phi'\left(\frac{T}{c}, \frac{H}{c}\right)$$

$$\frac{C_m(T, H)}{c} = \Phi'\left(\frac{T}{c}, \frac{H}{c}\right) \tag{11}$$

Similarly, the magnetization and susceptibility can be put into the form

$$\frac{M(T, H)}{c} = \zeta\left(\frac{T}{c}, \frac{H}{c}\right) \tag{12}$$

$$\chi(T, H) = \zeta'\left(\frac{T}{c}, \frac{H}{c}\right) \tag{13}$$

Equations (11) to (13) constitute what is now called "scaling laws" for the thermodynamical parameters of dilute spin-glasses such as AuFe, CuMn, and AgMn systems. Such laws of corresponding states do not predict the freezing phenomena observed in spin-glasses, they only underline what simple correspondences between the experimental quantities are expected when the concentration is changed. However, the reduced parameter T/c does imply that the freezing temperature is proportional to the concentration c if the former exists. So far, it seems that an interaction with alternating sign is sufficient

for the existence of the spin-glass ground state configuration at low temperature.

Let us recall the condition we established earlier for the scaling behavior to be observable. That is, the wavelength of the RKKY oscillation must be small compared to the inter-impurity distance. But how small? Experimentally, good agreement is obtained in alloys containing less than 1 at.% magnetic impurities (typical cases are AuFe, CuMn[16,17] and LaAuGd in P2). Using a value of ~ 6.9 for $2k_F a$, one obtains ~ 4 oscillating cycles separating two near-neighbor magnetic impurities. Thus, in order to observe the simple laws of corresponding states, it requires a statistical treatment of the $1/r^3$ interaction over at least 4 angular cycles (also see Fig. 7). Above 1 at.%, the interactions become more complicated due to clustering effects. In that case, there are preferential interactions of either sign. The simple scaling laws are no longer followed. Although in some special cases, like in our concentrated LaAuGd alloys, the statistical model of the remanent magnetization still works, as will be discussed in the next section. Sometimes, the more concentrated regime is called "mictomagnetic," meaning a complicated mixture of ferro- and antiferromagnetic interactions but without long-range order. We believe that similar fundamental physics (such as interactions, and anisotropy) are already contained in the dilute regime, and that the terminology is relatively unimportant. Hence we shall use the term "spin-glass" throught out discussion.

b. Summary of Experimental Results in Dilute Amorphous Alloys. Let us return to the original subject concerning the role of

electronic mean free path on the strength of magnetic interactions. First we have to ask: To what extent are the magnetic impurities interacting in our amorphous alloys? An answer is provided by the following experimental observations: (i) The magnetic properties follow the scaling predictions based on the assumption that the interaction has the form $1/r^3$. Moreover, the paramagnetic Curie temperature θ_p which measures the strength of the interaction is a monotonic increasing function of magnetic impurity concentration (P2). The latter fact is already contained in the scaling laws, while in a Kondo system θ_p is independent of concentration, as expected for a single-impurity effect. (ii) The depression of superconductivity at increasing magnetic impurity concentration discussed in P3 is very similar to that observed in magnetic superconductors where the impurities are interacting with each other. Thus the data presented in P2 and P3 can be analyzed in the same way as in the crystalline case. However, several authors who have treated the aforementioned subject theoretically[19, 43] all concluded that the indirect interaction would be severely damped off (more or less exponentially) as a function of distance in a disordered matrix, though the expressions they obtained differ somewhat from one another's. Unfortunately, there have been only a few experimental attempts to test these theories. Earlier study was made by Heeger et al[44] who observed a decrease in NMR linewidth when nonmagnetic impurities (which decrease the mean free path) were introduced into CuMn system (containing only 500 ppm Mn). Likewise, Souletie[45] studied the specific heats of AuFe doped with Ti. He checked the strength of the RKKY interaction based on the intuitive exponential law $e^{-r/\ell_{mfp}}$. He found that good agreement

was obtained when ℓ_{mfp} is greater than $2R_c$, the average distance separating the near-neighbor impurities. However, for $\ell_{mfp} < 2R_c$, the interaction became less and less attenuated. For example, when $\ell_{mfp} = R_c$ the interaction was 50% stronger than the theoretical value. However, one should be cautious about the possible effects of non-magnetic impurities on the magnetic moments, for Mn and Fe carry no moment when dissolved in Al and Ti respectively. In the previous studies, up to ~ 10% Al and ~ 5% Ti were dissolved in the normal matrices. This might affect the interactions among the magnetic impurities, possible through an attenuation of the magnetic moment. More recent investigations[46] were made on the depression of superconductivity in amorphous superconductors (In, Pb) doped with magnetic impurities (Mn). Comparison was then made with that in the crystalline counterpart. In the InMn system, the study was limited to 0.1 at.% Mn, since $T_c \sim 1.3°K$ at 800 ppm Mn. Comparison with the MHZ theory of Kondo superconductor seemed to indicate an attenuation in the magnetic interaction. For the PbMn alloys, the study can be extended to ~ 0.4 at.% Mn, but the results were contrary to those obtained by Petersen in Göttingen.[46]

c. Electronic Mean Free Path in Amorphous Metallic Alloys. In an amorphous alloy, what one can determine from the resistivity data is the diffusivity D_e as given in Eqn. (1), since the uncertainties in n and E_F are usually small. One is always tempted to evaluate the electronic mean free path ℓ_{mfp} from D_e using the free electron value of v_F. In some cases, it is found that the ℓ_{mfp} so determined is even smaller than an interatomic spacing. One then asks two

questions: Is the simple solution to the Boltzmann's transport equation applicable to amorphous metals? To what extent is the free electron model valid in these materials? We do not intend to deal with the first question in this thesis. Recently, Allen[47] pointed out that in random systems, successive scattering events are no longer independent of each other. The latter might lead to the inadequacy of the conventional Boltzmann equation. Under such circumstances, one can always refer to the exact solution of the Kubo transport equation. However, an equally difficult problem is involved since one needs to know the electronic eigenstates of the amorphous system. To justify indirectly the validity of the free electron model in these materials, one measures the Hall coefficient R_H and then compares it to the free electron value $R_o(= -1/ne)$.

In Table I, we listed for various amorphous metals the resistivity ρ, electronic mean free path ℓ_{mfp} evaluated from (1), the ratio of ℓ_{mfp} to the interatomic distance a, and the ratio of the Hall coefficient R_H to its corresponding free electron value R_o. One can see that whenever $R_H/R_o \simeq 1$, ℓ_{mfp} is on the order of a few interatomic spacings. The failure of the free electron model indicated either by a significant departure of R_H/R_o from unity or by a positive R_H (as in amorphous Mo) clearly leads to "anomalous" $\ell_{mfp}(\lesssim a)$. The tendency towards more localized electronic states would result in a lowering of v_F as compared to its free electron value. The "anomalous" ℓ_{mfp} might thus be easily underestimated by an order of magnitude.

TABLE I

Transport parameters of amorphous metals prepared by different techniques. The $La_{78}Au_{22}$ data are taken from Ref. 3. Others are taken from Ref. 2

	$\rho(10^{-4}\Omega cm)$	ℓ_{mfp}(Å)	ℓ_{mfp}/a	R_H/R_o
Ga	0.29	11.7	4.0	1.1
In	0.33	13.0	3.9	1.0
$Pd_{80}Si_{20}$ *	0.80	10.0**	3.7	~1.0
Sn	0.47	7.8	2.4	1.0
Bi	1.60	2.4	0.7	0.6
Pb	0.78	5.0	1.4	0.5
Mo	4.50	0.9***	0.3	negative
Tl	0.73****	6.2	1.8	-
$La_{78}Au_{22}$	2.50	1.8	0.5	-

* Values of ρ and R_H are taken from Ph.D. Thesis of R. D. Ayers (1971 , Caltech)

** Only two sp electrons are considered according to L. Ley and J. D. Riley, to be published in IEEE Trans. Mag. Sept. 1977

*** Counting only the s electrons

**** Determined for the liquid state

d. Attenuation of RKKY Interaction? DeGennes[19] pointed out that incoherent interference of the incident and scattered electronic waves in a disordered system would attenuate the RKKY interaction. He conjectured that the interaction in its asymptotic form is modified by an exponential factor $e^{-r/\ell}$. Other forms[19,43] of the attenuated RKKY interaction had also been proposed. Physically, the exponential factor comes from the spatial decay of the wavefunctions in a disordered matrix. Therefore, it is not clear that the transport mean free path is the relevant length to be included in the exponential decay. Since the former quantity results from a time dependent perturbation treatment (conductivity is a time dependent process), while the characteristic length ℓ_c which measures the range of the RKKY interaction should be related to the spin correlation length of the eigenstates in a disordered system. The relationship between these two fundamental quantities is not known up to this point. If $\ell_c \simeq \ell_{mfp} \simeq 10$ Å, the RKKY interaction given in (6) would be significantly modified in the dilute alloys. It follows that the geometrical arguments leading to the scaling laws discussed previously are no longer valid. In addition, it would also result in a more rapid depression of T_c in the Gd doped amorphous superconductors. Since it was observed beforehand from our experiments that such is not the case, one might tentatively conclude that $\ell_c > \ell_{mfp}$. Instead of solving the RKKY interaction in an amorphous matrix which requires a knowledge of the approximate electronic states of the system, we are at present satisfied with an estimate of the lower bound of ℓ_c which is consistent with our experimental observations. In the following discussion, we shall assume that the RKKY function has the asymptotic form $V(r)e^{-r/\ell_c}$.

It is possible to study the effect of amorphousness on the magnetic interactions by comparing the coupling strengths in dilute alloys to those in concentrated alloys. To be more specific, we have determined the strength of the RKKY interaction V_o in alloys containing less than 1 at.% Gd (P2) where the exponential factor is supposed to be important. Similar evaluation has also been made in the ferromagnetic $Gd_{80}Au_{20}$ alloys where the dominant contributions to the interaction are probably coming from only the first few nearest neighbors, and the effect of ℓ_c is thus less important. By comparing V_o obtained in the two extreme cases one is expected to obtain an estimate of ℓ_c. The average effect of ℓ_c on $V(r)e^{-r/\ell_c}$ which yields an attenuated V_o can be obtained by considering the half width of the molecular field distribution Δ. If the spins are oriented randomly in a matrix, statistical considerations imply that Δ is simply given by the root mean square molecular field acting on an average spin

$$\Delta^2\left(R_c/\ell_c\right) = \frac{4x}{d^3}\int_{R_c}^{\infty}\left[SV(r)e^{-r/\ell_c}\right]^2 \cdot 4\pi r^2 dr \qquad (14)$$

where x is the concentration of magnetic atoms, d is the lattice constant, and R_c is the average spherical volume containing one magnetic atom given by the expression

$$(16\pi/3) \times QR_c^3 = d^3 \qquad (15)$$

Q equals 1/4, 1/2, and 1 for the simple cubic, body-centered cubic, and face-centered cubic structure respectively. In general, one writes $\Delta = x S\gamma$ where γ (proportional to V_o in the clean limit) is the

parameter determined in experiments. Thus it is easy to show that $\gamma(R_c/\ell_c)$ is related to the unattenuated value $\gamma(o)$ by

$$\gamma(R_c/\ell_c) = \gamma(o)\left[3F_4(R_c/\ell_c)\right]^{\frac{1}{2}}$$

with

$$F_4(R_c/\ell_c) = \int_1^\infty \frac{\exp(-2R_c u/\ell_c)\,du}{u^4} \qquad (16)$$

A graphical representation of F_4 can be found in Ref. 45.

As will be discussed in a later section, the strength V_o for $Gd_{80}Au_{20}$ can be determined by using the DeGennes formula to be 0.5×10^{-37} erg cm^3. We have extended the interactions out to the sixth nearest neighbor without taking into account any attenuation effect. Such procedure is valid provided $\ell_c > 6a (\simeq 20\,Å)$. Moreover, the contributions from atoms located beyond the third nearest neighbor are small due to the intrinsic $1/r^3$ decay of the RKKY function. For the dilute alloys ($x \leq 1.0$), V_o (actually $\gamma(R_c/\ell_c)$) was determined to be 0.2×10^{-37} erg cm^3 according to P2. The latter yields a freezing temperature T_M of 0.33° K per at.% GD for the dilute spin glass. Experimentally, we obtained a value of 0.5° K per at.% Gd. The small discrepancy might come from the disagreement between the Ising and Heisenberg spin models. Here, we take $V_o = 0.29 \times 10^{-37}$ erg cm^3 in order to fit the experimental T_M values. We then obtain $\gamma(R_c/\ell_c) / \gamma(o) = 0.58$ which gives $R_c/\ell_c \simeq 0.35$ from (16). Taking $Q = \frac{1}{2}$ from structural data, and $x = 1$ at.%, we determine $R_c = 11 \cdot 8$ Å which gives $\ell_c \simeq 34$ Å. This value of ℓ_c is indeed much greater than

the transport mean free path ℓ_{mfp} in an amorphous matrix. For two magnetic atoms separated by a distance $2R_c$, the attenuation of the RKKY interaction only becomes important when $2R_c > \ell_c$. The latter corresponds to a concentration of $x < 0.2$ at.% Gd. Thus we can conclude that the scaling laws might be barely obeyed in our dilute alloys. One is expected to see significant departures from simple scalings at the thousand ppm range. This also suggests a consistent explanation for the previous experimental results obtained in dilute disordered crystalline alloys. As far as superconductivity is concerned, the critical concentration $x_{AG} \simeq 1$ at.% Gd is already too "high" for a significant depression of T_c. The exact meaning of the characteristic length ℓ_c awaits further theoretical investigations.

3. Determination of Freezing Temperature in Canonical Spin-Glasses

Experimentally, the freezing temperature T_M (some authors use T_g, T_o etc.) is defined as the temperature of the cusp in the susceptibility. Intensive effort has been taken to search for other possible anomalies in the Hall effect, Mössbauer effect, neutron scattering, NMR, and specific heat measurements. A well-defined freezing temperature T_M occurs in some of the measurements while only a broad change of behavior over a wide temperature range is observed in the others. In Table II, we summarize the various spin glass experiments conforming to these two classes of observations. This summary is based on a review article by Mydosh[14] in the Amorphous Magnetism II Symposium and has been updated since then. In this section, we focus on the determination of T_M using the mean field approximation (MFA). Various theories based on MFA produce

TABLE II

Collection of Experiments Relating to the Freezing Temperature

Well-defined T_M	Smeared Behavior
Susceptibility	Specific Heat
Remanence/Irreversibility	Resistivity
Mössbauer Effect	Thermoelectric Power
μ^+ - Precession	Ultrasonic Velocity
Nuclear magnetic resonance	

? Neutron Scattering ?

cusps in the specific heat C_m and susceptibility χ. Such a cusp in the specific heat has never been observed. However, one should recall that a MFA usually yields worse results for $C_m(T)$ than for $\chi(T)$ near a phase transition. In what follows, we shall first review the MFA treatment of the spin-glass problem. Then we shall compare the theoretical T_M values with the experimental values. By using the interaction strengths determined from high field magnetization measurements, it is shown that the RKKY force alone is sufficient to account for T_M in both canonical spin-glass alloys and alloys containing Gd atoms.

The spin-glass properties are apparently a consequence of the

interactions between the magnetic atoms. One can conceive different types of interactions, direct or indirect. The most interesting one being the RKKY interaction which has a unique spatial dependence leading to some kind of corresponding states. For mathematical reasons, the theorists are more willing to deal with a system containing a random distribution of magnetic component. The starting point is a Heisenberg or Ising Hamiltonian

$$H = - \sum_{j>i} J_{ij} \vec{S}_i \cdot \vec{S}_j + b \sum_i S_i^z \tag{17}$$

with $b = g\mu_B H$ and H is along the z axis; $J_{ij} = \left(|\vec{R}_i - \vec{R}_j| \right)$ is the exchange interaction. It has been accepted that for a spin-glass transition to occur, the interaction must have an alternating sign. The Hamiltonian in (17) is then used to evaluate the partition function from which other thermodynamic quantities can be derived. For fixed impurity configuration, a spin S_i will feel an internal field from its neighbors. Due to thermal activations on the spin system, the local field averages to zero if the average is taken over sufficiently long time at $T > T_M$

$$\langle \vec{S}_i \rangle = 0, T > T_M \tag{18}$$

where $\langle\ \rangle$ denotes thermal average. The basic concept for spin-glass is that there exists a well-defined temperature T_M below which all spins assume a fixed local axis since the local field at the lattice site i no longer averages to zero. That is

$$\langle \vec{S}_i \rangle \neq 0, \quad T < T_M \tag{19}$$

If the local axes are randomly distributed, the configurational average $\overline{\langle \vec{S}_i \rangle} = 0$ for all temperatures. In general, the static susceptibility for a system of N spins is given by the "fluctuation dissipation result"[24]

$$\chi = \chi_o \sum_{ij} \left[\langle \vec{S}_i \cdot \vec{S}_j \rangle - \langle \vec{S}_i \rangle \cdot \langle \vec{S}_j \rangle \right] / NS(S+1) \tag{20}$$

where $\chi_o = NS(S+1)g^2\mu_B^2 / 3k_B T$, the paramagnetic susceptibility for $T > T_M$. To evaluate (20), one can use a model in which the random distribution of impurity sites is replaced by a symmetric distribution in J_{ij}. With $P(J_{ij}) = P(-J_{ij})$ one can show that

$$\overline{\langle \vec{S}_i \cdot \vec{S}_j \rangle} = S(S+1)\delta_{ij}, \quad \overline{\langle \vec{S}_i \rangle \cdot \langle \vec{S}_j \rangle} = \overline{\langle S_i \rangle^2}\, \delta_{ij} \tag{21}$$

and we define $m^2 = \overline{\langle S_i \rangle^2}$ as the order parameter. For a classical Heisenberg model,

$$\chi = \chi_o \left[1 - m^2 \right] \tag{22}$$

In this approach, we have neglected the short-range correlations.

A theory which explains the sharp cusp in $\chi(T)$ by a sudden freezing of the impurity spins has been proposed by Edwards and Anderson[48] and extended by various authors.[49, 50] In these treatments short-range correlations are neglected. A self-consistent

equation for m^2 is derived from the configuration-averaged free energy. Both the classical Heisenberg model and the Ising model yield fairly similar results. Both the specific heat and susceptibility show a cusp at T_M. Calculations for a finite external magnetic field do indicate a rounded off effect on the cusps. Recent Monte-Carlo calculations[51] for the same model but avoiding the MFA yield a cusp in $\chi(T)$ and a broad maxima in $C_m(T)$. Thus the discrepancy with the experimental results seems to be due to the MFA, and not to the model. An approach based on the formation of clusters has been proposed by D. A. Smith.[52] A magnetic cluster is a connected group of spins which are coupled by exchange interactions with energy greater than the thermal energy. At decreasing temperatures, these clusters grow until the percolation limit is reached at some critical temperature T_M which is defined as the freezing temperature.

The simplest derivation for the order parameter m^2 in (21) is given by Sherrington.[50] Despite the simplicity of the mathematics involved, the expression for T_M thus obtained is in fairly good agreement with those obtained by more rigorous treatments.[48-50] One starts with the Hamiltonian in (17) by putting $b = 0$ and defines an order parameter $m = \overline{|\langle \vec{S}_i \rangle|}$. This definition of m is equivalent to that of (21) within the MFA. For a given distribution in J_{ij} the molecular field theory allows one to write

$$|\langle \vec{S}_i \rangle| = S\left|B_S\left(S\sum_{j>i} \hbar^2 J_{ij}\left|\langle \vec{S}_j \rangle\right| \cos\Phi_{ij}/k_B T\right)\right| \qquad (23)$$

where B_s is the Brillouin function and Φ_{ij} is the angle between $\langle \vec{S}_i \rangle$

and $\langle \vec{S}_j \rangle$. Around the spin-glass transition, the Brillouin function can be expanded as

$$|\langle \vec{S}_i \rangle| = \frac{S(S+1)}{3K_B T} \left| \sum_{j>i} \hbar^2 J_{ij} |\langle \vec{S}_j \rangle| \cos\Phi_{ij} + 0(\langle S \rangle^3) \right| \tag{24}$$

Iterating once

$$|\langle \vec{S}_i \rangle| = \left(\frac{S(S+1)}{3k_B T}\right)^2 \left| \sum_{j\ell} \hbar^4 J_{ij} J_{j\ell} |\langle \vec{S}_\ell \rangle| \cos\Phi_{j\ell} + O(\langle S \rangle^3) \right| \tag{25}$$

Assuming a random distribution of impurities and thus a symmetry distribution of J_{ij}, we retain only the $\ell = i$ terms on the right hand side of (25)

$$|\langle \vec{S}_i \rangle| = \left(\frac{\hbar^2 S(S+1)}{3k_B T}\right)^2 \overline{\left| \sum_j J_{ij}^2 |\langle \vec{S}_i \rangle| \cos^2 \Phi_{ij} \right|} \tag{26}$$

so that a nonzero solution exists at

$$T_M = \left[\hbar^2 S(S+1) / 3k_B\right] \overline{\left(\sum_j J_{ij}^2 \cos^2 \Phi_{ij} \right)^{\frac{1}{2}}} \tag{27}$$

Φ_{ij} obviously depends on the distribution of J_{ij}, if we assume J_{ij}^2 and $\cos^2 \Phi_{ij}$ can be averaged separately, we obtain

$$T_M = \left[\hbar^2 S(S+1)/ 3k_B\right] \overline{\left(\sum_j J_{ij}^2 \right)^{\frac{1}{2}}} \cdot \begin{cases} 1 \text{ Ising} \\ 1/\sqrt{3} \text{ Heisenberg} \end{cases} \tag{28}$$

We have taken $\overline{\cos^2 \Phi_{ij}}$ to be 1/3. The average $\overline{\left(\sum_j J_{ij}^2 \right)^{\frac{1}{2}}}$ is related to Δ by $\Delta = S\overline{\left(\sum_j J_{ij}^2 \right)^{\frac{1}{2}}}$. The leading behavior of m for $T \lesssim T_M$ follows

from examining the cubic term in (24). One then obtains

$$m^2 \alpha \left(T_M - T \right) \tag{29}$$

Combining (29) and (22) clearly yields a cusp at $T = T_M$. At $T > T_M$, $\chi(T)$ just becomes the Curie susceptibility $\chi_o(T)$.

By considering the temperature dependence of the thermal energy $U = -\frac{1}{2} \sum \hbar^2 J_{ij} \langle \vec{S}_i \rangle \cdot \langle \vec{S}_j \rangle$, one obtains a cusp at $T=T_M$ for the specific heat.

Our next task is to obtain an explicit expression for $\overline{\left(\sum_J J_{ij}^2 \right)}^{\frac{1}{2}}$ based on the RKKY interaction. Inserting the interaction of (5) and the critical radius R_c of (15) in (14), we perform the integration and obtain

$$\Delta = 11.8 \, S \, \Omega \, x \left(\frac{V_o}{d^3} \right) \tag{30}$$

Substitute (30) in (28) yields the freezing temperature T_M

$$T_M = \frac{11.8}{3} S(S+1) \, \Omega \, x \left(\frac{V_o}{d^3} \right) \cdot \begin{cases} 1 & \text{Ising} \\ 1/\sqrt{3} & \text{Heisenberg} \end{cases} \tag{31}$$

Thus knowing S and V_o, one can determine T_M. The values of V_o to be used in the following discussion are derived from high-field magnetization measurements as described in P2 and other experimental work cited therein. In Table III, we list the values of V_o, S, the theoretical Ising and Heisenberg values of T_M/x, and the experimental values of T_M/x for a series of dilute alloys. One should be reminded that the derivation of (31) is only valid for dilute magnetic components. At higher concentrations, one has to consider the correlation effects due to clustering which will be discussed in the next section. It can be seen that the experimental values of T_M/x

TABLE III

Comparison of theoretical and experimental values of T_M in dilute spin-glass alloys

Alloy	$V_o(10^{-37}$ erg cm$^3)$	S	T_M/x (°K/at.%)		
			Ising	Heisenberg	Expt.
CuMn	7.5	2.0	25.8	15.0	9.5 (a)
AgMn	3.5	2.0	8.5	4.9	4.5 (b)
AuMn	2.4	2.2	7.5	4.3	5.0 (a)
ZrMn	2.7	2.0	5.1	2.9	< 4.0 (c)
AuFe	11.0	1.5	14.7	8.5	9.3 (d)
LaAuGd	0.4	3.8	1.2	0.7	0.5 (e)
La_3InGd	-	3.5	-	-	0.6 (f)
LaGd	-	3.5	-	-	0.5 (f)

(a) V. Cannella in Amorphous Magnetism, edited by H. O. Hooper and A. M. De Graaf (Plenum, N.Y. 1973) p. 195

(b) V. Cannella and J. A. Mydosh, AIP Conference Proceedings 18, 651 (1974)

(c) H. C. Jones et al, to be published in August 1, Phys. Rev. (1977)

(d) Reference 17 and others cited therein

(e) Present work

(f) R. P. Guertin, J. E. Crow, and R. D. Parks, Phys. Rev. Lett. 16, 1095 (1966): D. K. Finnemore, L. J. Williams, F. H. Spedding, and D. C. Hopkins, Phys. Rev. 176, 712 (1968)

agree well with the theoretical Heisenberg values. However, it should be noted that the derivation of V_o is based on the Ising model. It is not clear that the Heisenberg model would give similar values. Recently, a computer model of spin-glass[53] using the Heisenberg Hamiltonian is simulated. By fitting the specific-heat data at low temperatures, it is found that the value of V_o obtained is just slightly smaller than the Ising value. There is also a definite relationship between the strength of the RKKY interaction and the magnitude of T_M. As is well-known, the weakness of such an indirect exchange interaction in rare-earth alloys originates from the localization of 4f electrons in Gd. The latter is also responsible for the smaller T_M values.

Finally, it should be mentioned that other interactions such as dipolar force between magnetic atoms and the presence of crystal field can also influence the freezing phenomena. As will be discussed in a later section, dipolar interaction is responsible for the remanence phenomena. However, it is usually two orders of magnitude smaller than the RKKY interaction and thus it is too weak to affect T_M. On the other hand, crystal-field anisotropy can be as large as the RKKY force and thus it can affect T_M significantly. A recent study on ScGd and ScTb systems clearly illustrates this point.[54] The single-ion anisotropy is absent in alloys containing Gd. Thus we have demonstrated that in an ideal case (i.e., dilute alloys, normal matrix, and absence of crystal-field effect), spin-glass freezing can be accounted for by the isotropic RKKY force alone.

B. SPIN-GLASS ALLOYS CONTAINING HIGH Gd CONTENT ($1.25 < x < x\ 70$)

1. Phenomenology

In this section, we present a qualitative discussion of our experimental results. Alloys in this region are characterized by susceptibility maxima in low-field measurements (Fig. 8) and the thermomagnetic history effects (isothermal and thermal remanent magnetization as shown in P4). The dependence of T_M on Gd concentration is illustrated in Fig. 9. It can be seen that T_M varies linearly with x for alloys containing less than 12 at.% Gd. At higher concentrations, T_M increases more rapidly with x. The $T_M(x)$ dependence will be discussed in a more quantitative fashion later. It is clear from Fig. 8 that the peaks in $\chi(T)$ are reduced and rounded off in small applied fields. They disappear in samples cooled in fields greater than ~ 1 kOe. In Fig. 10 are shown the $\chi^{-1}(T)$ data taken over a wide temperature range for these alloys. The paramagnetic regions are clearly established at sufficiently high temperatures giving a well-defined paramagnetic Curie temperature θ. This value of $\theta(\simeq 3\ T_M)$ is found to increase with x indicating a stronger trend towards ferromagnetic coupling. The large values of $\theta - T_M$ also indicate the presence of ferromagnetic clusters around T_M. The latter implies that the spin-glass phenomena in these alloys are probably due to the freezing in of the ferromagnetic clusters in their local field below T_M. This conjecture allows us to understand both the freezing mechanism and the variation of T_M. Using the classical

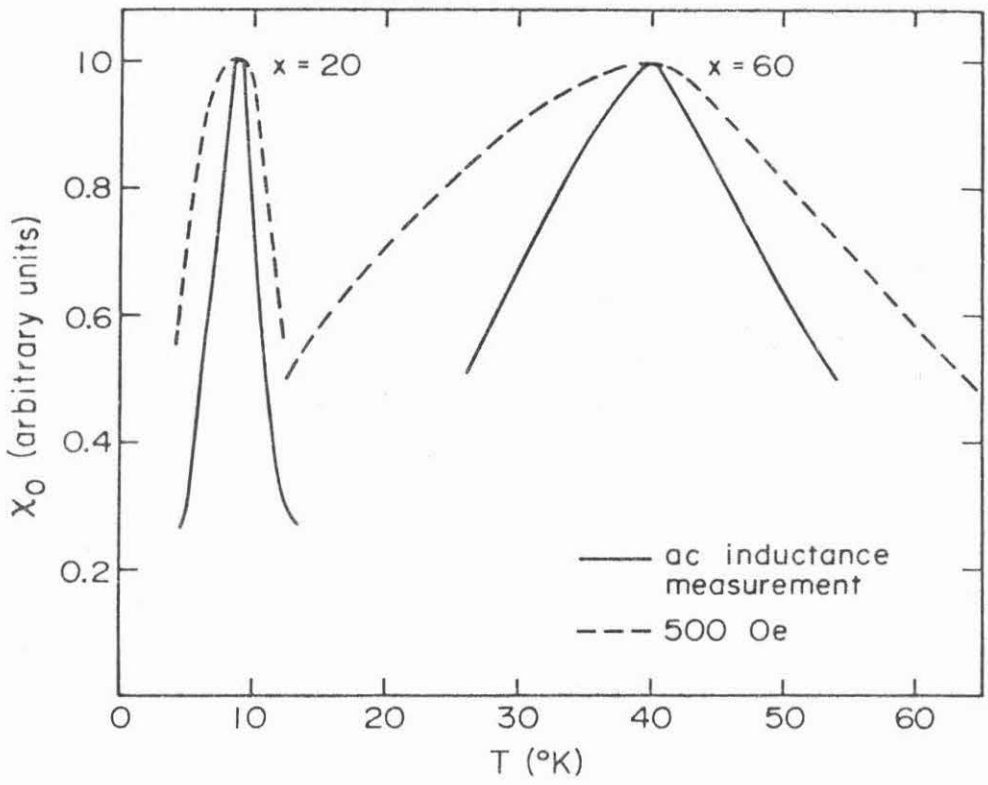

Fig. 8. Susceptibility (in arbitrary units) vs. temperature measured in zero field and in 500 Oe for x = 20 and 60 samples.

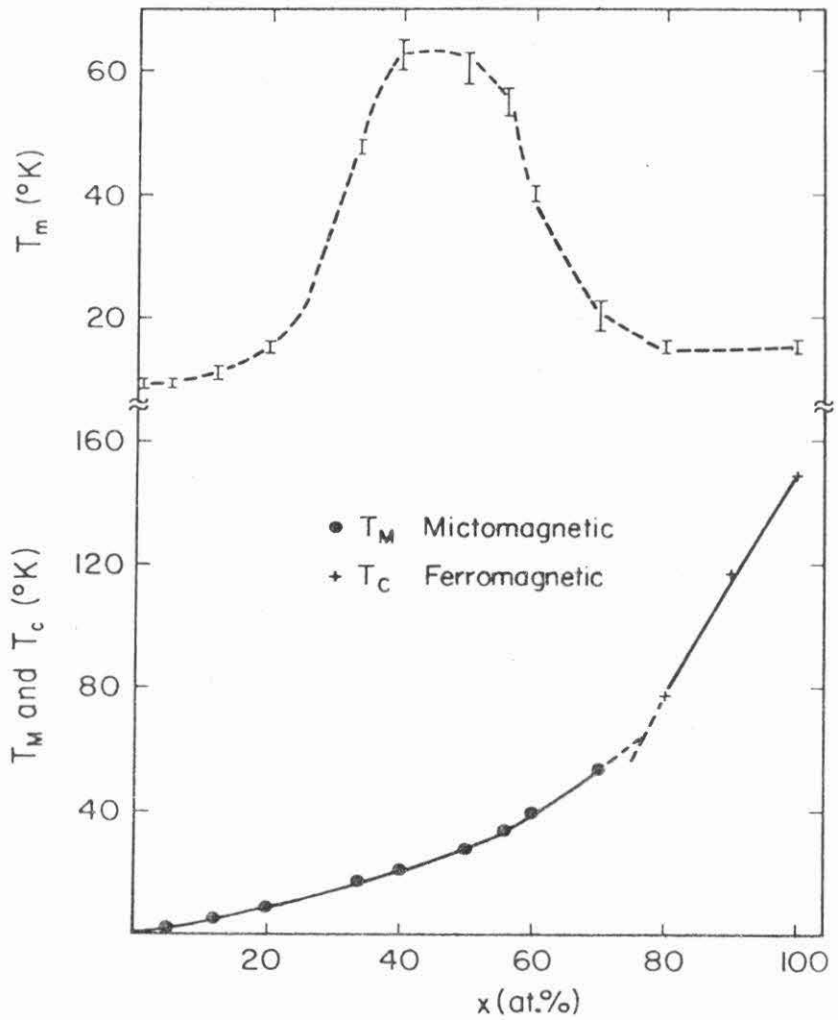

Fig. 9. Magnetic phase diagram of $(La_{100-x}Gd_x)_{80}Au_{20}$ indicating the freezing temperature T_M and Curie temperature T_c as a function of x. The compositional dependence of resistivity minima T_m is also included.

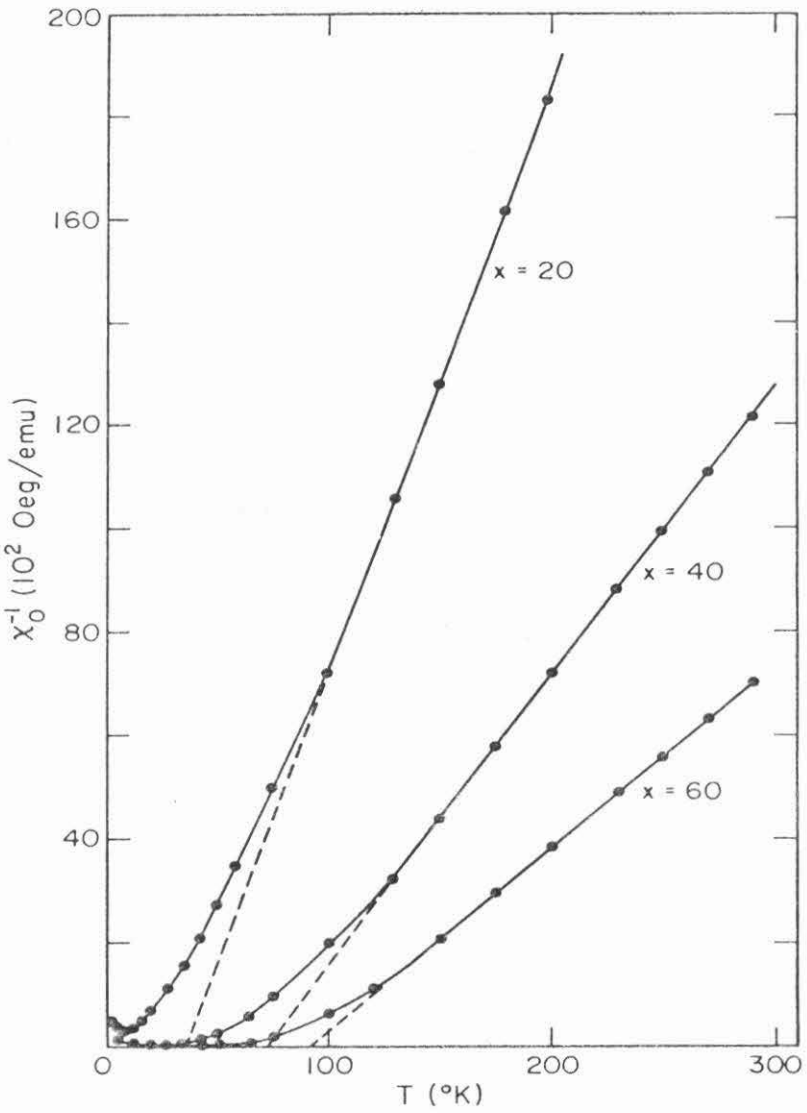

Fig. 10. Reciprocal susceptibility vs. temperature for the x = 20, 40 and 60 alloys. High temperature sections are extrapolated to give C_{CW} and θ.

molecular field approach, the effective number of Bohr magnetons per Gd atom is found to remain constant and close to the value 8 which corresponds to the ionic value 7.94.

In Fig. 11, we show the low-temperature magnetization data for the $x = 20$ sample measured in fields up to 70 kOe. The difficulty of saturating the Gd moment at low temperature is rather obvious. Using the magnetization data, the classical Arrott plots (M^2 vs. H/M) are obtained. Such plots for two samples ($x = 40$, 60) are shown in Fig. 12. Strong departures from linearity at small and high fields at temperatures below θ are seen, so that any spontaneous magnetization and Curie temperature cannot be defined. However, the $M^2(H/M)$ isotherms are observed to approach closer to the M^2-axis for higher Gd concentrations indicating a gradual onset of spontaneous magnetization for $x > 70$. The absence of spontaneous magnetization from the Arrott plots for all $T < \theta$ also points towards the possibility of weak and inhomogeneous ferromagnetic interactions. For temperatures between T_M and θ, the superparamagnetic clusters break up gradually at increasing temperature to yield single magnetic moments above θ.

Resistivity minima are observed over the whole concentration range for $x > 0.6$. At very low concentrations, the fluctuation conductivity above T_c probably washes out the enhanced resistivity at low temperature. The variation of the resistivity minima (T_m) follows a bell-shaped curve as shown in Fig. 9. A plausible explanation for the occurrence of resistivity minima in concentrated alloys is given in P5. It is suggested that the resistivity minima in

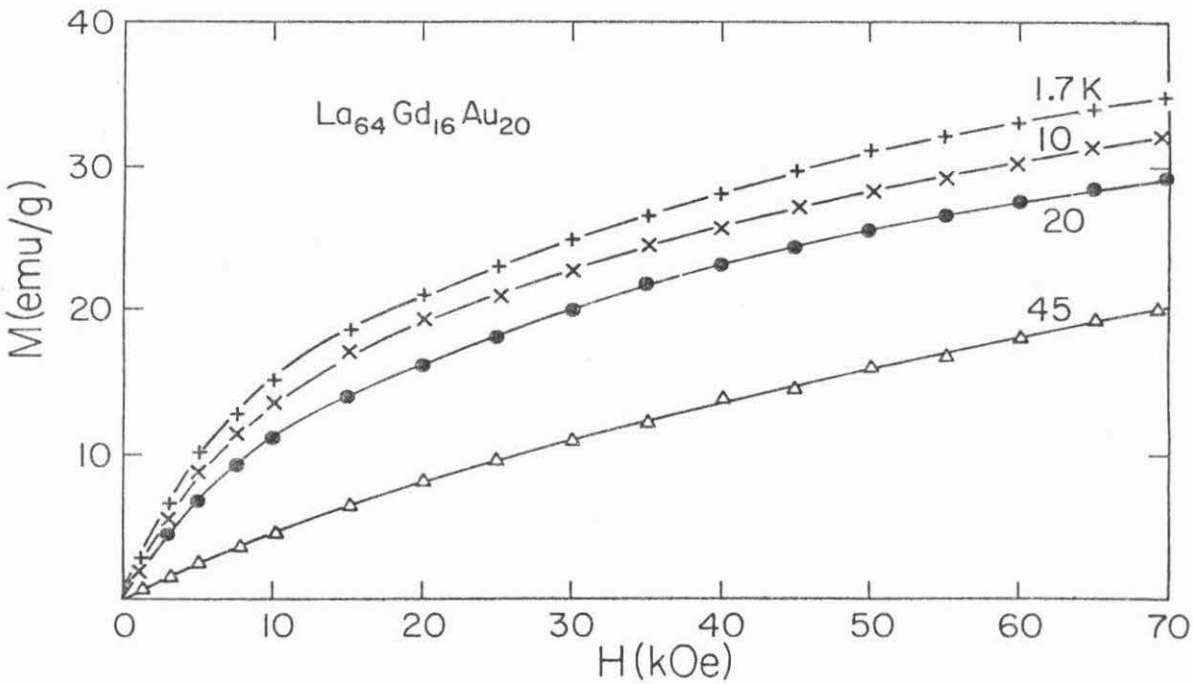

Fig. 11. Magnetization vs. applied field for $La_{64}Gd_{16}Au_{20}$.

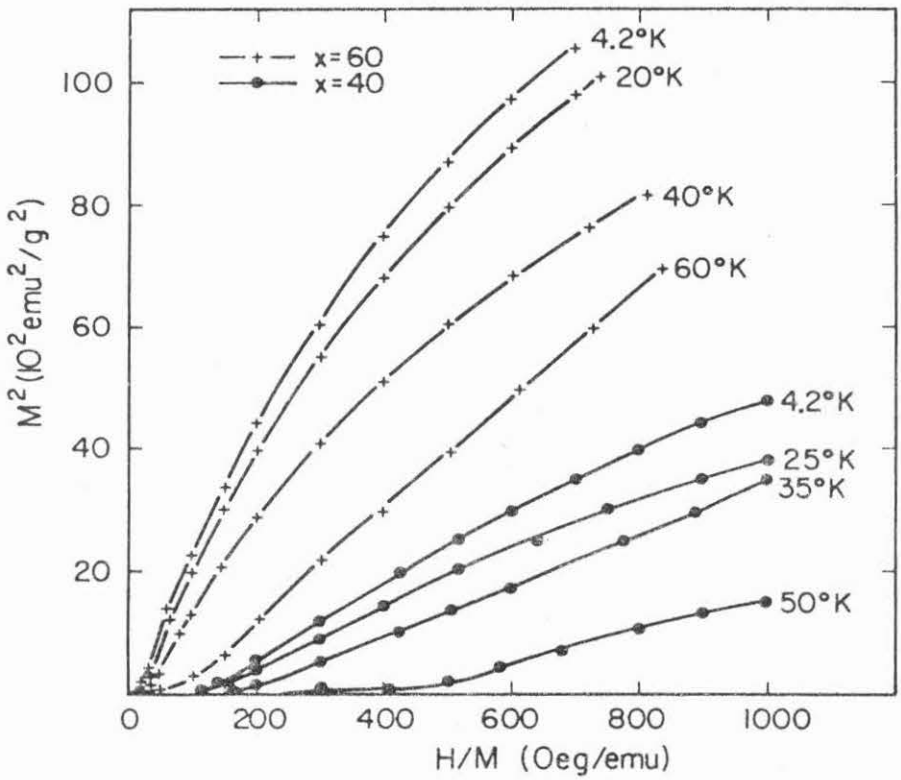

Fig. 12. Arrott plots for x = 40 and 60 samples from 4.2K to temperatures above T_M.

these alloys are caused by a mechanism of electron scattering from magnetic clouds coupled by the RKKY interaction. We will show in the next section that this conjecture is also consistent with the explanation for the occurrence and the magnitude of the spin-glass transition temperature T_M. Moreover, it is also observed that the variation of the coefficient of the A(x) log T term in $\rho(T)$ also exhibits a similar curve as $T_m(x)$ in Fig. 9. This dependence of A(x) resembles the theoretical prediction of Kaneyoshi and Honmura.[55] The latter authors suggested a bell-shaped curve of A(x) based on the percolation problem.

2. A Phenomenological Model for Spin-Glass Mechanism in Gd Concentrated Alloys

In dilute spin-glass alloys[16,17] containing less than 1 at.% magnetic component, the freezing temperature T_M varies linearly with the concentration x. For higher concentrations[14], T_M varies as some power law x^m where $m \neq 1$. In the latter case, the direct exchange interactions become important and we have to consider clustering effects. We can treat the clusters (can be antiferromagnetic, chemical, ferromagnetic, etc.) as single spin entities interacting with each other through random forces. We can use a model in which the distribution of the size of clusters is given by a probability function, such as Gaussian or Lorentzian. Or we can use a mathematically simpler approach in which all the clusters are of the same size. In what follows, we will take the latter approach to study the variation of T_M above the dilute regime. It will be shown that the main features of the magnetic phase diagram can be obtained

by simple arguments. In particular, the model predictions are compared with the experimental results obtained by us and other authors.

Taking the clusters as single spin entities each carrying a moment S^*S, the concentration of clusters as x^*, and the average RKKY interaction between the clusters as V_o^*, one obtains an expression similar to (31)

$$T_M = \frac{11.8}{3\sqrt{3}} S^{*2} Q x^* \left(\frac{V_o^*}{d^3}\right) S^2 \tag{32}$$

with $x^* = x/n$, n being the number of spins within a cluster. The moment S^* is given by

$$S^* = n^p , \qquad p < 1 \tag{33}$$

taking into account that the clusters might not carry the full moment due to some misalignments of the spins. Next, we attempt to derive an expression for the effective interaction V_o^* between the clusters from a statistical argument. We derive the second moment of the field distribution Δ^2 from two viewpoints. First, considering the interaction $V^*(r)$ between the clusters, then rather straightforwardly we obtain

$$\Delta^2 \propto x^{*2} S^{*2} S^2 V_o^{*2} \tag{34}$$

Next, we consider the interaction V(r) between individual spins in the

matrix. Since the spins within a cluster are strongly correlated, therefore they are likely to flip collectively. The effective concentration of spin is reduced to x^* and we then obtain

$$\Delta^2 \propto x^{*2} S^2 V_o^2 \tag{35}$$

Comparing (34) and (35) yields

$$S^* V_o^* = V_o \tag{36}$$

and an expression for T_M

$$T_M = \frac{11.8}{3\sqrt{3}} S^2 Q \left(\frac{x}{n^{1-p}}\right)\left(\frac{V_o}{d^3}\right) \tag{37}$$

Now we consider different cases:

(i) If the spins within the clusters are ferromagnetically coupled, then $p \approx 1$ and $T_M \propto x$.

(ii) If some of the spins within a cluster are coupled antiferromagnetically, then $p < 1$, $T_M \propto x/n^{1-p}$. Since it is likely that n is an increasing function of x, say $n(x) \propto x^q$, therefore $T_M \propto x^m$ with $m = 1 - q(1-p) < 1$. In the case of complete antiferromagnetic coupling within clusters, the net moment S^* is just given by the surface contribution, that is $p = 2/3$. Then $m = 1 - \frac{q}{3}$.

It should be noted that the above argument is valid as long as (36) holds. This requires that the distribution of local field be

random or equivalently the size of the clusters be small. Obviously, the latter condition is satisfied in not too concentrated alloys. As we will see later, an experimental criterion is that the remanent magnetization can at most be a few percent of the saturation magnetization. We will focus on this point in a moment. It is observed[14] in typical spin-glass alloys CuMn, AgMn, AuFe, etc., that T_M varies as x^m where $0.55 < m < 0.75$ for $1 < x < 10$. It is known that Mn tends to form antiferromagnetic clusters in a normal matrix. Thus our conclusion (ii) seems reasonable. It would be interesting to check the variation of cluster sizes as a function of Mn concentration in the range $1 < x < 10$.

In order to determine the freezing temperature of concentrated LaAuGd alloys (i.e., $x > 1$) from (32), one has to know the variation of S^*, x^*, V_o^* as a function of x. Two sets of measurements are taken, namely the magnetization $M(H,T)$ and magnetoresistivity $\rho(H,T)$ experiments. As discussed in P5, both the $M(H,T)$ and $\rho(H,T)$ data can be fitted to a modified Brillouin function of the form $B_{S^*}\left(\mu^* H/k_B(T+\theta_c)\right)$ where the notations are self evident. As emphasized beforehand, such fittings are phenomenological without sound theoretical basis. However, it allows us to obtain approximate values of the cluster sizes and the characteristic temperatures θ_c. A typical result is shown in Fig. 13. We plotted the values of S^* determined by both approaches in Fig. 14. In the same figure, we included a schematic variation of the first nearest neighbors coordination shell (defined by the Gd-Gd nearest neighbors) obtained by extrapolating the RDF results[56] on amorphous $La_{80}Au_{20}$. By comparing the values of S^*

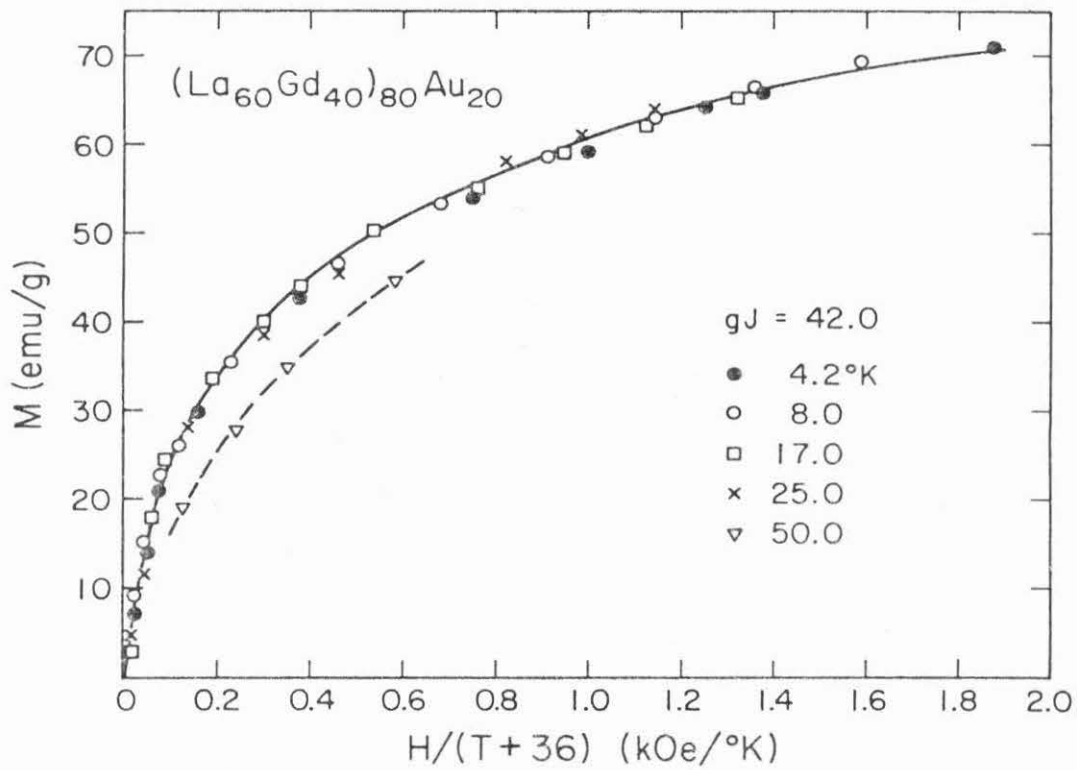

Fig. 13. Magnetization vs. H/(T + 36) for the x = 40 alloy. Solid line is a Brillouin function fit with g = 2, J = 21 and θ_c = 36K. The dashed line indicates deviation from this relation at higher temperatures.

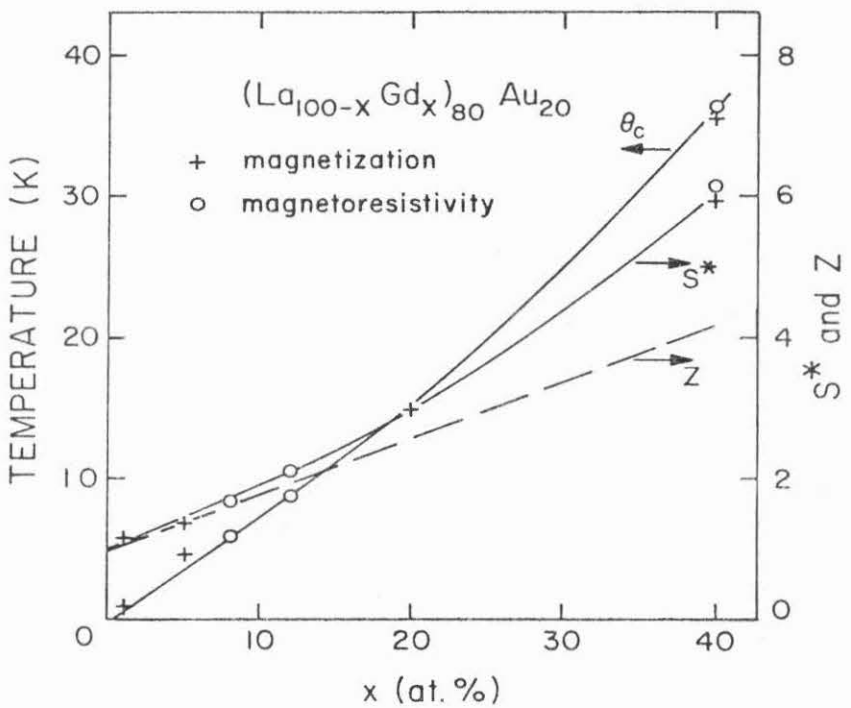

Fig. 14. Compositional dependence of θ_c, S^* and Z. The notations are defined in the text.

and Z, one can say that for $x < 20$, the size of coordination shell determined the size of magnetic clusters. For higher Gd content, $S^* > Z$ indicating the interactions become more complicated. Above $x = 40$, it is no longer possible to analyze the magnetization data using a Brillouin function. It is also seen that θ_c varies linearly with x. One should distinguish between θ_c determined from $H > 10$ kOe to the low field θ mentioned earlier. We believe that θ_c originates from the inter-clusters interaction while θ arises from intra-cluster interaction. The former quantity is positive in sign which resembles those obtained in dilute alloys where the RKKY interaction is dominant. The latter quantity is negative in sign which describes the "strength" of the ferromagnetic interaction within a cluster. The above argument is further supported by the fact that the freezing temperature $T_M \simeq \theta_c$ (Figs. 9 and 14). Thus we tentatively conclude that the freezing phenomena are determined by the inter-clusters interaction. Furthermore from the fact that $\theta \simeq 3\ T_M$, the intra-cluster correlation is stronger than the inter-clusters correlation. To first order approximation, we just assume $S^*(T_M) = S^*$ in the following discussion.

The strength of interaction V_o^* can be determined at low temperature and high field using a modified form of equation (1) in P2

$$M(H,T) = x^* g\mu_B S^* S \left[1 - \frac{2(2S^*S+1)\, x^*\, V_o^*}{3g\mu_B H} - \frac{A^* k_B T}{H} \right] \qquad (38)$$

Using similar plots as in P2, one obtains $(2S^*S+1)\, V_o^*$ from which one determines V_o^* knowing S^*. A typical plot of equation (38) is shown

in Fig. 15 for the x = 5 alloys. The values of V_o^* so determined are normalized by V_o determined for the dilute alloys x < 1. From magnetoresistivity measurement, we obtain V_o^* for three alloys using Eqn. (3) of P5. Seven normalized values of V_o^* are shown in Fig. 16. To test the validity of (36) (i.e., $V_o^* S^* = V_o$), we also plotted the curve $V_o^*/V_o = 1/S^*$ using the values of S^* determined earlier. It can be seen that (36) is well satisfied. Taking p = 1 for ferro-clusters, we obtain a linear dependence of T_M on x using Eqn. (37). However, according to Fig. 9, $T_M \propto x^m$ with m > 1 for x > 15. Fig. 17 gives a log-log plot of T_M vs. x from which one obtains m = 1.3 for x > 15. Our model predicts the correct form of $T_M(x)$ for x < 15 which is in good agreement with conclusion (i) but it gives lower T_M values for x > 15. It is rather unlikely that the $T_M(x)$ dependence at high concentration is due to a mean free path effect, as we have shown that such an effect is even unimportant for x ≃ 1. We suggest that for high concentrations, the S^*-clusters dissociate into smaller clusters at T_M as shown schematically in Fig. 18. The smaller clusters have larger values of V_o^* which contribute to a higher T_M value for a given concentration of magnetic component. Therefore what we can conclude is that for ferro-clusters, $T_M(x)$ is at least linear. For clusters with "missing" moments, conclusion (ii) implies that $T_M(x)$ exhibits negative deviation from linearity, as exemplified by the CuMn, AgMn and AuMn systems.

Next, we consider the origin of remanent magnetization in our alloys. The experimental data and analysis have been given in P4. Here, we remark that the phenomena can be explained in terms

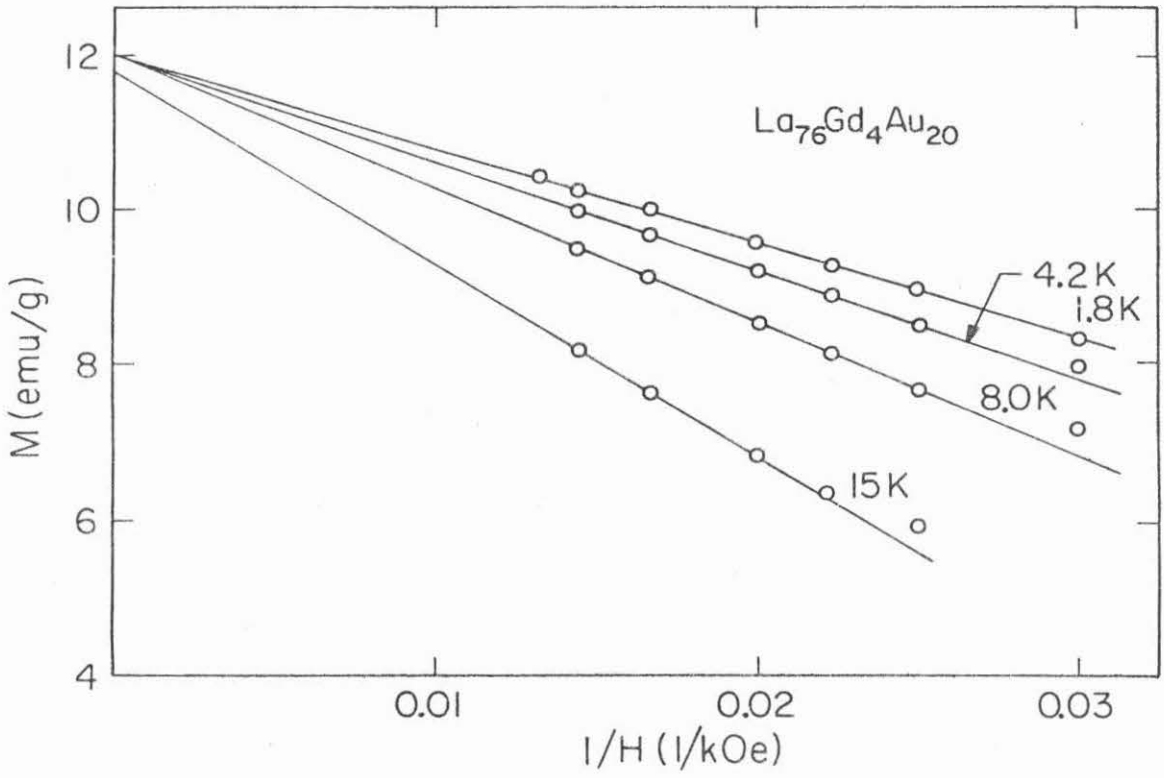

Fig. 15. Magnetization vs. reciprocal field for the x = 5 alloy at low temperatures.

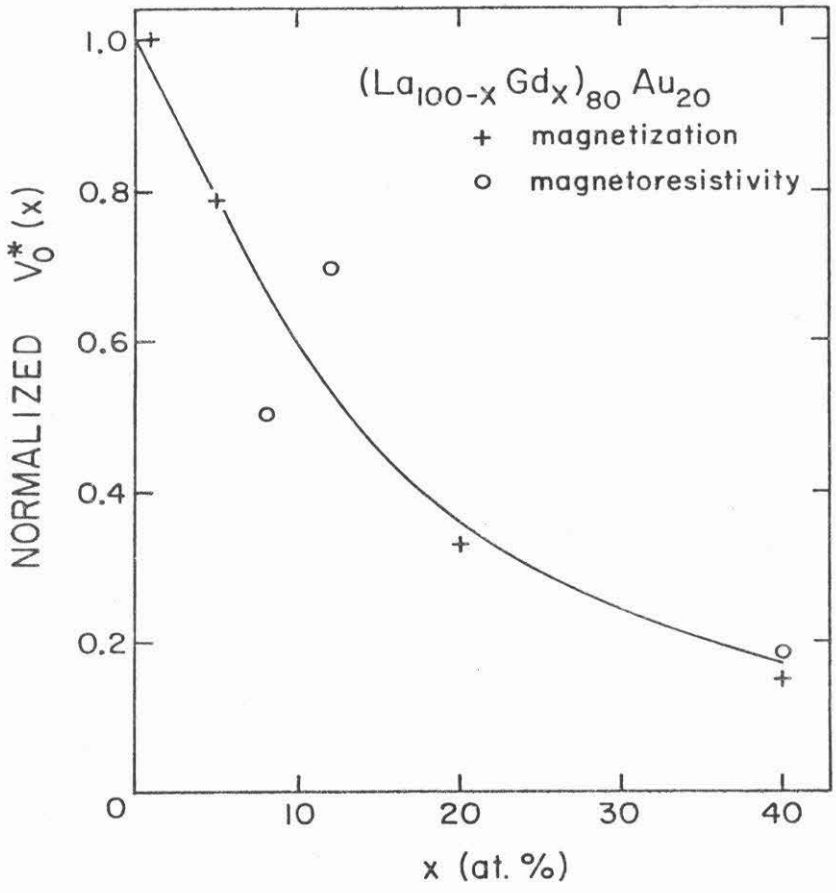

Fig. 16. Compositional dependence of the normalized strength of interaction. Solid line is a plot of $1/S^*(x)$.

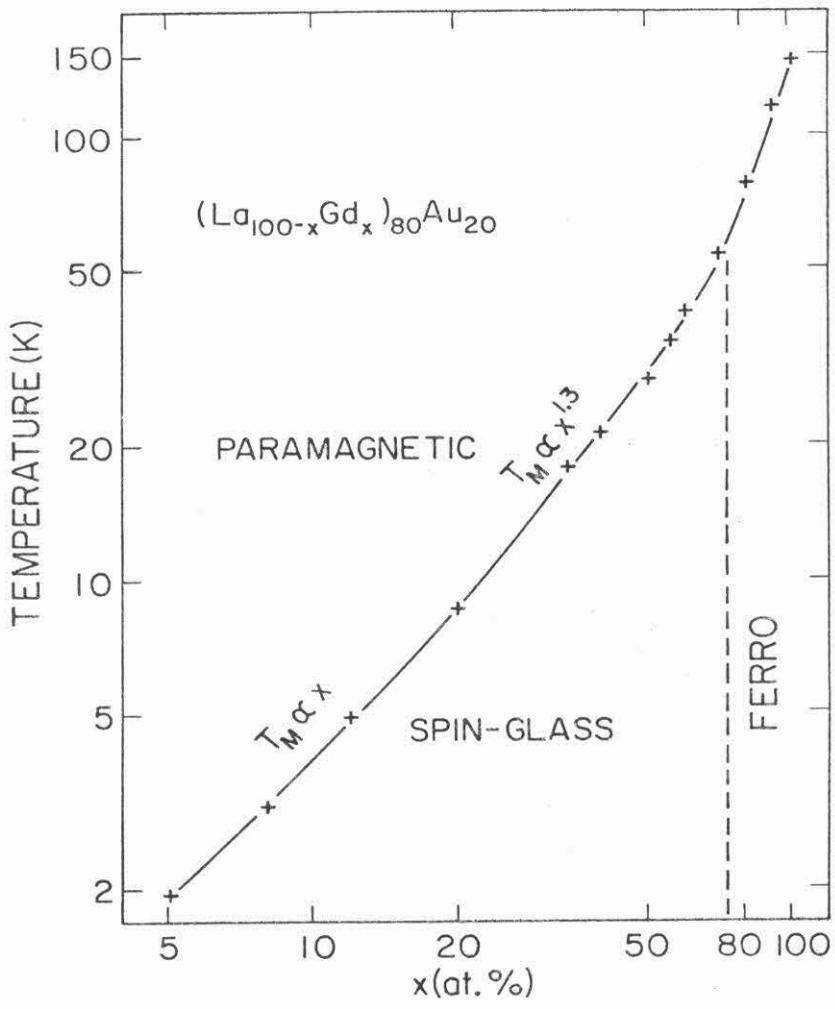

Fig. 17. Transition temperature vs. composition on log-log plot.

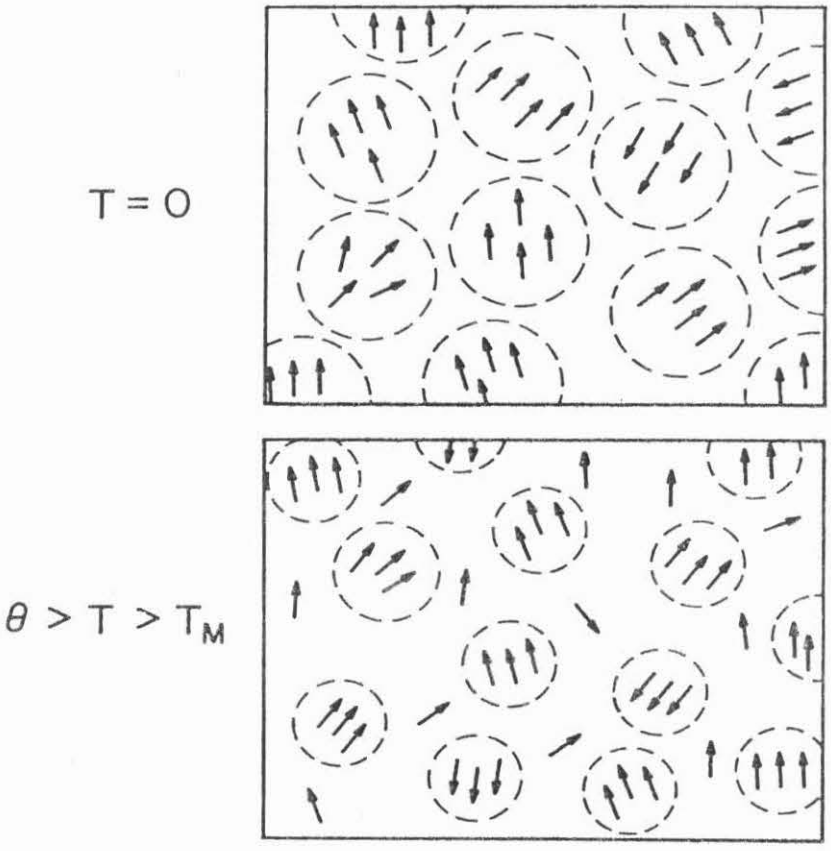

Fig. 18. Schematic pictures of magnetic clusters at T = 0 and their dissociation into smaller clusters above T_M but below θ.

of ferro-clusters as single spin entities interacting through the dipolar and RKKY forces. To conserve the number of spins, we have $x^* = N_o n_o$, where n_o is the number of clusters in a cloud and N_o is the concentration of clouds in at.%. Similar to P4

$$n_o = \frac{1}{2\pi} \left(M_{\infty}(0) / M_{rs}(0) \right)^2 \tag{39}$$

The half width of the RKKY field distribution Δ_{KB} is given by expression (34). For the dipolar field width Δ_d, one can carry out the same derivation as for V_o^* in (36) to obtain a similar reduction in the strength of the inter-clusters dipolar interaction. Hence it is easy to see that

$$n_o = \Delta_{KB} / \Delta_d \approx V_o \tag{40}$$

even for concentrated alloys, as illustrated by our data. It is interesting to note that at lower concentrations (e.g., $x < 5$), $\Delta_{KB} \alpha x$. For higher concentrations, Δ_{KB} no longer increases linearly with x. Instead, there is a trend for Δ_{KB} to saturate. From (35), $\Delta^2 \alpha x^{*2}$. But $x^* = x/S^*$ which remains essentially constant for $5 < x < 40$ when S^* increases with x. We emphasize again that the "random field approximations" we have been using in this section in deriving expression (32) to (37) is favored by the smallness of the ratio $M_{rs}(0) / M_{\infty}(0) \simeq 0.05$ in concentrated alloys. Since $\Delta_{KB}/\Delta_d \simeq 50$, the dipolar force is responsible for the remanent magnetization but it is too weak to yield a susceptibility maximum. The relationship of M_{rs} to T_M only comes from an energy balance between the dipolar

force and RKKY force. We have shown that the RKKY force alone is sufficient for explaining the magnitude of T_M up to $x \simeq 40$. The analysis in our system is simplified by the absence of enhanced matrix and crystal-field anisotropy effects. It also suggests that an additional anisotropy (in this case the dipolar force) is needed to account for the remanence phenomena.

C. FERROMAGNETIC ALLOYS ($70 < x < 100$)

1. Onset of Ferromagnetism

Alloys in this regime are characterized by a well-defined Curie temperature. The magnetic phase transition determined from ac inductance bridge measurements gives a transition width of ~ 10° K. The Curie temperature is defined by the inflection point on the signal intensity versus temperature curve. The spontaneous magnetization can be determined either from the Arrott plots or modified Arrott plots as discussed fully in P6. Nonlinearity in M^2 vs. H/M is observed indicating inhomogeneities in ferromagnetic couplings. This is also supported by the fact that the inflection point on the M(H) vs. T plots disappears in fields greater than 2kOe. The temperature domain over which ferromagnetic inhomogeneities dominate narrows as x increases until at $Gd_{80}Au_{20}$ $(\theta_p - T_c)/T_c \simeq 0.1$. The variation of the mean magnetic moment per atom when La is substituted for Gd obeys fairly well a dilution law.

One might attribute the high critical concentration for long-range ferromagnetic order (~ 60 at.% Gd) to the amorphous structure of the alloys, since the percolation thresholds are ~ 25 at.% using a

closed-packed structure of 8 rare-earth nearest neighbors. In the case of RKKY interaction, one expects a simpler problem than in the case of transition metals where the d-d overlap is important. However, several experimental facts disagree with such a conjecture. In amorphous Gd-Ag and Gd-Cu[57] alloys, the onset of ferromagnetism already starts at $\lesssim$ 30 at.% Gd. While in the case of amorphous Gd-Al alloys[57], the alloy containing ~ 37 at.% Gd is still a spin-glass. Not to mention the crystalline case, such variation in the critical concentration suggests an important role played by the second constituent in the alloys. In fact, the indirect exchange interaction (usually referred to as super-exchange interaction) among the Gd spins mediated by a second atomic species in which antiferromagnetic alignments are favored might be important.[57] This is thought to be the case in quite a number of Gd alloys and compounds where the saturation moments are found to be smaller than that in pure Gd. For comparison with transition metal alloys, a percolation theory based solely on the RKKY interaction is still desirable. It is also worth mentioning that in amorphous transition metal alloys[58], the theoretical percolation limits are obeyed, indicating the relatively unimportant role played by the amorphous structure in determining the critical concentration.

Recently, Tahir-Kheli[59] used CPA to study ferromagnets with simultaneous site and (isotropic) exchange bond disorders. He analyzed the structure of the interfaces between ferromagnetic, spin-glass and paramagnetic phases of such a system. It was found that in order to have a spin-glass phase persisting up to ~ 60 at.%

magnetic components, the fluctuation in the exchange constant has to be as large as the mean exchange constant.

IV. SUMMARY AND CONCLUSION

We have studied the electrical and magnetic properties of a series of amorphous La-Gd-Au alloys prepared by splat cooling. These alloys are obtained by complete substitution of Gd for La in the $La_{80}Au_{20}$ matrix. The $La_{80}Au_{20}$ alloys are ideal type II superconductors with a transition temperature (T_c) of 3.5° K. In the dilute regime (less than 1 at.% Gd), the magnetic properties of the alloys are typical of those observed in canonical spin-glasses where the magnetic atoms are interacting with each other through the indirect RKKY exchange force. Meanwhile, close to the critical concentration for the disappearance of superconductivity, the superconducting transition temperatures exceed those predicted by the Abrikosov-Gor'kov theory. The latter gives additional manifestation of magnetic interaction among impurities and also suggests the possible coexistence of superconductivity and spin-glass freezing. In the superconducting state, the freezing phenomena might be quite different from those in the normal state since the electronic structures are modified below T_c. Thus it would be interesting to measure the freezing temperatures (T_M) in the superconducting state.

We have discussed the role of amorphousness on the magnetic interactions. Conventionally, the transport mean free path ($\ell_{mfp} \sim 5$ to 10Å) has been used to estimate the attenuation of the RKKY interaction in a disordered matrix. This concept, when applied to an amorphous matrix is found to be inconsistent with the experimental results. Instead, a characteristic length ℓ_c of ~ 30Å can account for

the variation of the strength of RKKY interaction ranging from the dilute regime ($\gtrsim$ 0.2 at.% Gd) to the concentrated regime (> 60 at.% Gd). The physical meaning of ℓ_c is probably related to the spin correlation length of the electronic states, or equivalently the mean free path for conduction-electron spin polarization in the matrix. The relationship between ℓ_c and ℓ_{mfp} awaits further theoretical investigation. To check the magnitude of ℓ_c experimentally, one should study the magnetic properties in the more dilute regime ($\lesssim$ 1000 ppm).

We have used the theories of Edwards, Anderson and Sherrington to explain the occurrence of T_M in various canonical spin-glass systems. The strength of the RKKY interaction is determined from high field magnetization measurements. It is found that the RKKY force alone can in general account for the magnitude of T_M in these systems and also in our La-Gd-Au alloys. As is rather common for any mean field treatment, a better agreement between experiment and theory is usually obtained for the susceptibility than for the specific-heat results in phase transitions. This is also true for spin-glass alloys. We have extended the mean field theory to the concentrated La-Gd-Au alloys. Clustering effects are taken into account by considering the magnetic clusters as single spin entities interacting via random forces. In our alloys, this approach is further simplified by the absence of enhanced matrix and crystal field effects. The fundamental quantities (such as the strength of interaction and size of clusters) are derived from magnetization and magnetoresistance experiments. The values of T_M can be accounted for this way. Although the situation is probably more complicated in

other alloy systems, the results of the present study suggest that an additional anisotropic interaction (e.g., dipolar force) is required for the remanence in our alloys. But the dipolar force is too weak to account for the freezing in of spins. Recent Monte Carlo calculations without mean field approximation are able to reproduce a sharp cusp in the susceptibility and a smeared behavior in the specific heat. It would be appropriate to perform specific heat measurements on our alloys which provide a simple spin system for comparison with magnetization measurements.

REFERENCES

1. W. Buckel and R. Hilsch, Z. Phys. 138, 109 (1954); Z. Phys. 138, 136 (1954)

2. G. Bergmann, Phys. Reports 27C, 159 (1976)

3. W. L. Johnson, S. J. Poon and P. Duwez, Phys. Rev. B11, 150 (1975); W. L. Johnson and S. J. Poon, J. Appl. Phys. 46, 1787 (1975); W. L. Johnson and S. J. Poon, IEEE Trans. on Mag., Mag. 11, 189 (1975)

4. W. Buckel and R. Hilsch, Z. Phys. 128, 324 (1950)

5. B. T. Matthias, H. Suhl, and E. Corenzwit, Phys. Rev. Lett. 1, 92 (1958)

6. A. A. Abrikosov and L. P. Gor'kov, Zh. Eksp. Teor. Fiz. 39, 1781 (1960); [Sov. Phys.—JETP 12, 1243 (1961)]

7. For a review of this subject, see M. B. Maple, in Magnetism V, Rado and Suhl edit., p. 289 (Academic Press, New York, 1973); also in Appl. Phys. 9, 179 (1976)

8. E. Müller-Hartmann, in Magnetism V, Rado and Suhl edit., p. 353 (Academic Press, New York, 1973); J. Zittartz, A. Bringer, and E. Müller-Hartmann, Solid State Commun. 10, 513 (1972) and references cited therein

9. K. H. Benneman and J. W. Garland, Intern. J. Magnetism 1, 97 (1971)

10. P. Entel and W. Klose, J. of Low Temp. Phys. 17, 529 (1974)

11. D. Rainer, in Low Temperature Physics LT13, Vol. 2, p. 593, Timmerhause et al edit. (Plenum Press, New York-London 1974); also in Z. Phys. 252, 174 (1972)

12. D. Davidov, K. Baberschke, J. A. Mydosh and G. J. Nieuwenhuys, J. Phys. F: Metal Phys. 7, L47 (1977)

13. S. J. Poon and J. Durand, Solid State Commun. 21, 999 (1977)

14. For a review of this subject, see J. A. Mydosh, AIP Conf. Proc. 24, 131 (1975); also in 2nd Int. Symp. on Amorphous Magnetism, Troy, N.Y. (1976)

References, (Cont'd)

15. M. A. Ruderman and C. Kittel, Phys. Rev. 96, 99 (1954); T. Kasuya, Prog. Theor. Phys. 16, 45 (1956); K. Yosida, Phys. Rev. 106, 893 (1957)

16. A. Blandin, Thesis, University of Paris (1961); J. Souletie and R. Tournier, J. Low Temp. Phys. 1, 95 (1969); A. I. Larkin and D. E. Khmel'nitskii, Zh. Eksp. Teor. Fiz. 58, 1789 (1970) [Sov. Phys.-JETP 31, 958 (1970)]

17. J. L. Tholence and R. Tournier, J. Phys. (Paris) 35, C4, 229 (1974); F. Holtzberg, J. L. Tholence and R. Tournier, in 2nd Int. Symp. on Amorphous Magnetism, Troy, N.Y. (1976); F. W. Smith, Phys. Rev. B14, 241 (1976) and references by the same author cited therein.

18. B. V. B. Sarkissian and B. R. Coles, Commun. Phys. 1, 17 (1976); M. H. Bennett and B. R. Coles, Physica 86-88B, 944 (1977)

19. P. G. de Gennes, J. Phys. Radium 23, 630 (1962); T. Kaneyoshi, J. Phys. F5, 1014 (1975)

20. See the reviews of P. A. Beck, Met. Trans. 2, 2015 (1971); R. Tournier, in LT13, Boulder, Colo., 1972, Timmerhaus et al edit. (Plenum Press, New York, 1974) Vol. 2, p. 257; B. R. Coles, in Amorphous Magnetism, Hooper and de Graaf edit. (Plenum Press, New York, 1973), p. 169

21. T. E. Sharon and C. C. Tsuei, Phys. Rev. B5, 1047 (1972); A. Zentko, P. Duhaj, L. Potochi, T. Tima and J. Bansky, Phys. Stat. Solidi (a) 31, K41 (1975); R. C. Sherwood, E. M. Gyorgy, H. J. Leamy, and H. S. Chen, AIP Conf. Proc. 34, 325 (1976)

22. M. E. Fisher, Phys. Rev. 176, 257 (1968); A Brooks Harris, J. Phys. C7, 1671 (1974); A. Brooks Harris and T. C. Lubensky, Phys. Rev. Lett. 33, 1540 (1974); T. C. Lubensky and A. B. Harris, AIP Conf. Proc. 24 311 (1975); V. Krey, Phys. Lett. 51A, 189 (1975); G. Grinstein and A. Luther, Phys. Rev. B13, 1329 (1976); H. Muller-Krumbhaar, J. Phys. C9, 345 (1976) and ref. cited therein

23. T. Mizoguchi, AIP Conf. Proc. 34, 286 (1976); K. Yamada, Y. Ishikawa, Y. Endoh, and T. Masumoto, Solid State Commun. 16, 1335 (1975); E. Figueroa, L. Lundgren, O. Beckman, and S. M. Bhagat, Solid State Commun. 20, 961 (1976); L. J. Schowalter, M. B. Salamon, C. C. Tsuei and R. A. Craven, APS Bulletin 22, AL4, March (1977)

24. See for example, H. E. Stanley, in "Introduction to Phase Transitions and Critical Phenomena," (Oxford University Press, New York and Oxford, 1971); M. Vicentini-Missoni, J.M. H. Levelt Sengera, and M. S. Green, J.Res. Nat'l. Bus. Std. 73A, 563 (1969). For more recent reviews, see M. E. Fisher, Rev.Mod. Phys. 46, 597 (1974); L. P. Kadanoff, in "Phase Transition and Critical Phenomena," edited by C. Domb and M. S. Green, (Academic, New York, 1976) Vol. 5A, p. 18,

25. A. I. Gubanov, Fiz. Taverd, Tela 2, 502 (1960), [Soviet Physics-Solid State 2, 468 (1961)]; K. Handrich, Phys. Stat. Solidi 32, K55 (1969), also (b) 53, K17 (1972); J. Schreiber, S. Kobe, K. Handrich, and J. Richter, Phys. Stat. Solidi (b) 70, 673 (1975); T. Kaneyoshi, J. Phys. C6, L19 (1973)

26. R. A. Tahir-Kheli, in "Phase Transition and Critical Phenomena," edited by C. Domb and M. S. Green, (Academic Press, New York, 1976) Vol. 5B, p. 259; A. B. Harris, P. L. Leath, B. G. Nickel, and R. J. Elliot, J. Phys. C7, 1693 (1974); J. Schreiber, Phys. Stat. Solidi (b) 59, K119 (1973)

27. R. Harris, M. Phischke, and M. J. Zuckermann, Phys. Rev. Lett. 31, 160 (1973); J. Phys. (Paris) 35, C4, 265 (1974)

28. M. N. Deschizeanx and G. Develey, J. Phys. (Paris) 32, 319 (1971); H. E. Nigh, S. Legvold, and F. H. Spedding, Phys. Rev. 132, 1092 (1963); C.D. Graham, Jr., J. Appl. Phys. 36, 1135 (1965)

29. J. S. Kouvel and J. B. Comly, Phys. Rev. Lett. 20, 1237 (1968). J. S. Kouvel and D. S. Rodbell, Phys. Rev. Lett. 18, 215 (1967). A. Arrott and J. E. Noakes, Phys. Rev. Lett. 19, 786 (1967)

30. J. Hopkinson, Philos. Trans. R. Soc. Lond. A180, 443 (1889); D. J. Dunlop, J. Geophys. Res. 40, 439 (1974)

31. E. P. Wohlfarth, Philos. Trans. R. Soc. Lond. A240, 599 (1948); L. Neél, Ann. Geophys. 5, 99 (1949)

32. J. S. Kouvel, J. Phys. Chem. Solids 21, 57 (1961); J. Owen, M. E. Brownes, V. Arp, and A. F. Kip, J. Phys. Chem. Solids 2, 85 (1957); O. S. Lutes and J. L. Schmit, Phys. Rev. 125, 433 (1962)

33. J. S. Kouvel, J. Phys. Chem. Solids 24, 795 (1963) and refs. cited therein; Michael W. Klein, Phys. Rev. 132, 2412 (1963)

34. V. Cannella and J. A. Mydosh, Phys. Rev. B6, 4220 (1972)

35. P. Duwez, in "Progress in Solid State Chemistry" (Pergamon, Oxford and New York, 1966), Vol. 3, p.377

36. G. Tangonan, Ph.D. Thesis, Caltech (1975)

37. W. L. McMillan, Phys. Rev. 167, 331 (1967)

38. W. L. Johnson and C. C. Tsuei, Phys. Rev. B13, 4827 (1976); and private communication

39. W. H. Shull and D. G. Naugle, APS Bulletin, FJ11, March, 1977; and private communication

40. F. H. Spedding and J. J. Croat, J. Chem. Phys. 59, 2451 (1973)

41. A. Blandin and J. Friedel, J. Phys. Radium 20, 160 (1959). B. Caroli, J. Phys. Chem. Solids 28, 1427 (1967)

42. Baruch Fisher and Michael W. Klein, Phys. Rev. B14, 5018 (1976); Physica 86-88B, 863 (1977)

43. A. Madhukar, J. Phys. (Paris) C4, 295 (1974)

44. A. J. Heeger, A. P. Klein, and P. Tu, Phys. Rev. Lett. 17, 803 (1966)

45. J. Souletie, Ph.D. Thesis, Grenoble (1968)

46. G. Zimmermeyer and B. Roden, Z. Physik B24, 377 (1976). W. Bauriedl and G. Heim, Z. Physik B26, 29 (1977)

47. Philip B. Allen, Phys. Rev. Lett. 37, 1638 (1976)

48. S. F. Edwards and P. W. Anderson, J. Phys. F: Metal Phys. 5, 965 (1975)

49. K. H. Fisher, Solid State Commun. 18, 1515 (1976), also in Phys. Rev. Lett. 34, 1348 (1975)

50. D. Sherrington and B. W. Southern, J. Phys. F: Metal Phys. 5, L49 (1975); D. Sherrington, J. Phys. C: Solid State Phys. 8, L208 (1975); D. Sherrington and S. Kirkpatrick, Phys. Rev. Lett. 35, 1792 (1975)

51. K. Binder and K. Schroder, Solid State Commun. 18, 1361 (1976); also in Phys. Rev. B14, 2142 (1976); K. Binder, Z. Phys. B26, 339 (1977)

52. D. A. Smith, J. Phys. F: Metal Phys. 4, L266 (1974); 5, 2148 (1975)

53. L. R. Walker and R. E. Walstedt, Phys. Rev. Lett. 38, 514 (1977)

54. B. V. B. Sarkissian, J. Phys. F: Metal Phys. 7, L139 (1977)

55. T. Kaneyoshi and R. Honmura, Phys. Lett. 46A, 1 (1973). T. Kaneyoshi, Phys. Status Solidi (b) 66, K1 (1974)

56. J. Logan, Scripta Metallurgica 9, 379 (1975)

57. See references cited in P6

58. See for example, T. E. Sharon and C. C. Tsuei, Phys. Rev. B5, 1047 (1972) and their previous work cited therein

59. R. A. Tahir-Kheli, Solid State Commun. 19, 1213 (1976)